Author Contributions:
Conceptualization: M. E. Gibson, M. J. Pound
Data curation: M. E. Gibson, J. McCoy
Formal analysis: M. E. Gibson, J. McCoy
Funding acquisition: J. M. K. O'Keefe, M. J. Pound
Investigation: M. E. Gibson, J. McCoy
Methodology: M. E. Gibson, J. McCoy, M. J. Pound
Project Administration: J. M. K. O'Keefe, N. B. Nuñez Otaño, S. Warny, M. J. Pound
Software: M. E. Gibson

Reconstructing Terrestrial Paleoclimates: A Comparison of the Co-Existence Approach, Bayesian and Probability Reconstruction Techniques Using the UK Neogene

M. E. Gibson[1], J. McCoy[1], J. M. K. O'Keefe[2], N. B. Nuñez Otaño[3], S. Warny[4], and M. J. Pound[1]

[1]Department of Geography and Environmental Sciences, Northumbria University, Newcastle upon Tyne, UK, [2]Department of Physics, Earth Science, and Space Systems Engineering, Morehead State University, Morehead, KY, USA, [3]Laboratorio de Geología de Llanuras. Facultad de Ciencia y Tecnología, Universidad Autónoma de Entre Ríos, Sede Diamante, CONICET (National Scientific and Technical Research Council), Buenos Aires, Argentina, [4]Department of Geology & Geophysics, and Museum of Natural Science, Center for Excellence in Palynology, Louisiana State University, Baton Rouge, LA, USA

Abstract Neogene sediments in the UK are ideally situated for understanding the early development of hydrological dynamics and atmospheric circulation that led to the modern oceanic climate of northwest Europe. Onshore Neogene fossiliferous deposits in the UK are limited to the solution pipe fills at Trwyn y Parc in Anglesey (Middle Miocene), the Brassington Formation of Derbyshire (Serravallian-Tortonian), and the Coralline Crag Formation (latest Zanclean-earliest Piacenzian) and Red Crag Formation (Piacenzian-Gelasian) in southeast England. Palynoflora from these localities can be used to provide snapshots into the climate at the time of deposition, however, palaeobotanical-based reconstructions are typically lacking in their poor estimation of error. Therefore, we present the first pre-Quaternary application of two terrestrial climate reconstruction techniques: CREST (Climate Reconstruction SofTware) and CRACLE (Climate Reconstruction Analysis using Coexistence Likelihood Estimation), that use Bayesian and likelihood estimation probability respectively to generate a new palaeoclimate reconstruction, and compare this to Co-existence Approach reconstructions from the UK and continental Europe. Our study shows how Mean Annual Temperature (MAT) declines by 3°–6°C, Mean Annual Precipitation (MAP) declines by 480–600 mm and Precipitation Seasonality approximately halves throughout the Neogene. CREST and CRACLE reconstructions overlap with the Co-exisence Approach and have the advantage of providing uncertainty, rather than ranges. The UK appears to have had a milder, wetter, and less seasonal climate than continental Europe. This is likely due to the buffering effects of the Atlantic Ocean and North Sea ameliorating the UK Neogene climate despite regional and global changes in atmospheric and oceanic circulation.

1. Introduction

1.1. Rationale

Little is known about the development of the modern oceanic climate regime of northwest Europe in deep time. During the Neogene (23.03–2.588 Ma), the British Isles had a unique location on the northwest edge of the Eurasian continent forming a peninsula separating the Atlantic Ocean from the North Sea (Harzhauser & Piller, 2007). Neogene sediments of the UK are therefore ideal for understanding the development of Neogene oceanic climates.

The modern European climate experiences a prevalence of the westerlies in winter with summer climates being highly latitudinally diverse. Western coastal areas, such as the UK, experience an oceanic, or maritime, climate with highly latitudinally diverse summer climates relative to southern Europe with its Mediterranean climate and dry summers and the subhumid-semi-arid continental climate of eastern Europe (Rohli & Vega, 2008; Vines, 1985). However, during the late Middle Miocene (Serravallian, 13.82–11.62 Ma) summer precipitation patterns suggest Europe was instead dominated by a trade wind system flowing from the northeast to southwest, whilst the Late Miocene was controlled by the westerlies (Böhme, 2004; Quan et al., 2014). However, much of this work is based upon the central European basins and does not, potentially, reflect terrestrial environments with a strong oceanic control. In addition, the majority of terrestrial paleoclimate reconstructions are generated through the Co-existence Approach (Burls et al., 2021; Utescher et al., 2014). Whilst this has given us unprecedented understanding of terrestrial climate development (e.g., Utescher et al., 2017), the reconstruction of a

Supervision: M. J. Pound
Validation: M. J. Pound
Visualization: M. E. Gibson
Writing – original draft: M. E. Gibson, M. J. Pound
Writing – review & editing: M. E. Gibson, M. J. Pound

range of equal probability presents challenges in direct comparison with climate model simulations (range vs. uncertainty; Salzmann et al., 2013). In this paper we present the first pre-Quaternary application of two terrestrial climate reconstruction techniques CREST (Climate Reconstruction SofTware) and CRACLE (Climate Reconstruction Analysis using Coexistence Likelihood Estimation) that use Bayesian and coexistence likelihood-based probability respectively, to provide a new paleoclimate reconstruction for the Neogene of the UK.

Despite the Miocene climate having been extensively studied in Europe (Bruch et al., 2011; Popova et al., 2012, 2013; Utescher et al., 2017) little is known about the specifics of the early development of hydrological dynamics and atmospheric circulation (Bruch et al., 2011; Eronen et al., 2012; van Dam, 2006). Furthermore, nearest living relative-based reconstructions from palaeobotanical data are typically lacking in their poor estimation of statistical error. Here we reconstruct the temperature and hydrological dynamics of the UK climate throughout the Neogene using three different nearest living relative techniques. The Co-existence Approach is the most common analytical approach for deriving quantitative palaeoclimate data from pre-Quaternary palynological data (Utescher et al., 2014). However, the Co-existence Approach reconstructs a range for each palaeoclimate parameter that complicates comparisons with other proxy-based reconstructions and climate model outputs. Statistical techniques can be applied to nearest living relative data to determine a probable mean and uncertainty (e.g., Klages et al., 2020). Herein, we apply two easy to run R-based scripts CREST (Chevalier et al., 2014) and CRACLE (Harbert & Nixon, 2015) which are compared to the widely applied Co-existence Approach to show the applicability of these techniques to pre-Quaternary palaeobotanical data and to examine the development of oceanic climates compared to European continental climates during the Neogene.

1.2. Neogene of the UK

The Neogene is subdivided into two epochs, the Miocene (23.03–5.333 Ma) and Pliocene (5.333–2.588 Ma). The British geological record is not replete with onshore deposits of Miocene and Pliocene fossiliferous strata (Figure 1), especially relative to the equivalent deposits offshore and in continental Europe (King, 2016; Mosbrugger et al., 2005) due to large-scale plate tectonic processes which have caused localized basin inversion and widespread exhumation of the Miocene landscape, as well as Quaternary glacial processes (Lee et al., 2018). Onshore Miocene deposits in the UK are limited to solution hollows, an outlier and weathered residues. The oldest dated sediments come from the solution pipe fills at Trwyn y Parc in Anglesey (Walsh et al., 1996) which have recently been reassigned to a Middle Miocene, possibly Langhian age (Pound & McCoy, 2021). The Brassington Formation, a succession of terrestrial sands, gravels and clays infilling karstic cavities in the southern part of the Lower Carboniferous Peak Limestone Group outcrop of the Peak District of Serravallian to Tortonian age (Pound & Riding, 2016; Walsh et al., 2018), is the most extensive onshore Miocene deposit in the UK. The Lenham Formation in southeast England is tentatively dated to the latest Miocene—earliest Pliocene based on its molluscan fauna and stratigraphical position, but has not yielded palynomorphs (King, 2016). The aeolian/colluvial deposits of the St. Agnes Outlier in Cornwall has yielded a depauperate pollen flora that has allowed a Miocene age assignment (Walsh et al., 1987). Weathering horizons in northeast Scotland have also been assigned to the Middle Miocene (Hall et al., 2015). The Pliocene onshore deposits outcrop in the southeast of England and comprise of shallow marine sediments, represented by the Coralline Crag Formation a (latest Zanclean— earliest Piacenzian; Andrew & West, 1977; King, 2016) and the Red Crag Formation represents a 600–800 kyr time window in the latest Pliocene (Piacenzian-Gelasian; Davies et al., 2019; Head, 1998; Lee et al., 2018; Riding et al., 2000).

Miocene palynology from Trwyn y Parc and the Brassington Formation show the presence of subtropical to warm-temperate forests in the UK (Pound & McCoy, 2021; Pound & Riding, 2016; Pound, Riding, et al., 2012). Terrestrial climates have previously been reconstructed for the UK using the Co-existence Approach (Pound & McCoy, 2021; Pound & Riding, 2016; Pound, Riding, et al., 2012). These results imply limited cooling from the Langhian of Trwyn y Parc to the Serravallian of the Brassington Formation (Pound & McCoy, 2021; Pound & Riding, 2016). This was tentatively interpreted as being the result of a tempering influence from a warm North Atlantic current (Denk et al., 2013; Pound & McCoy, 2021). No temperature difference was reconstructed between the Serravallian and early Tortonian of the Brassington Formation, but a shift in the seasonality away from a summer-wet climate (Pound & Riding, 2016). This was proposed to relate to a shift in atmospheric circulation (Pound & Riding, 2016; Quan et al., 2014). A cooling of mean annual temperature was reconstructed from the early to late Tortonian of the Brassington Formation of 1°–3°C, accompanied by decreases in both winter and summer temperatures (Pound & Riding, 2016) as well as a reduction in seasonality (Pound & Riding, 2016).
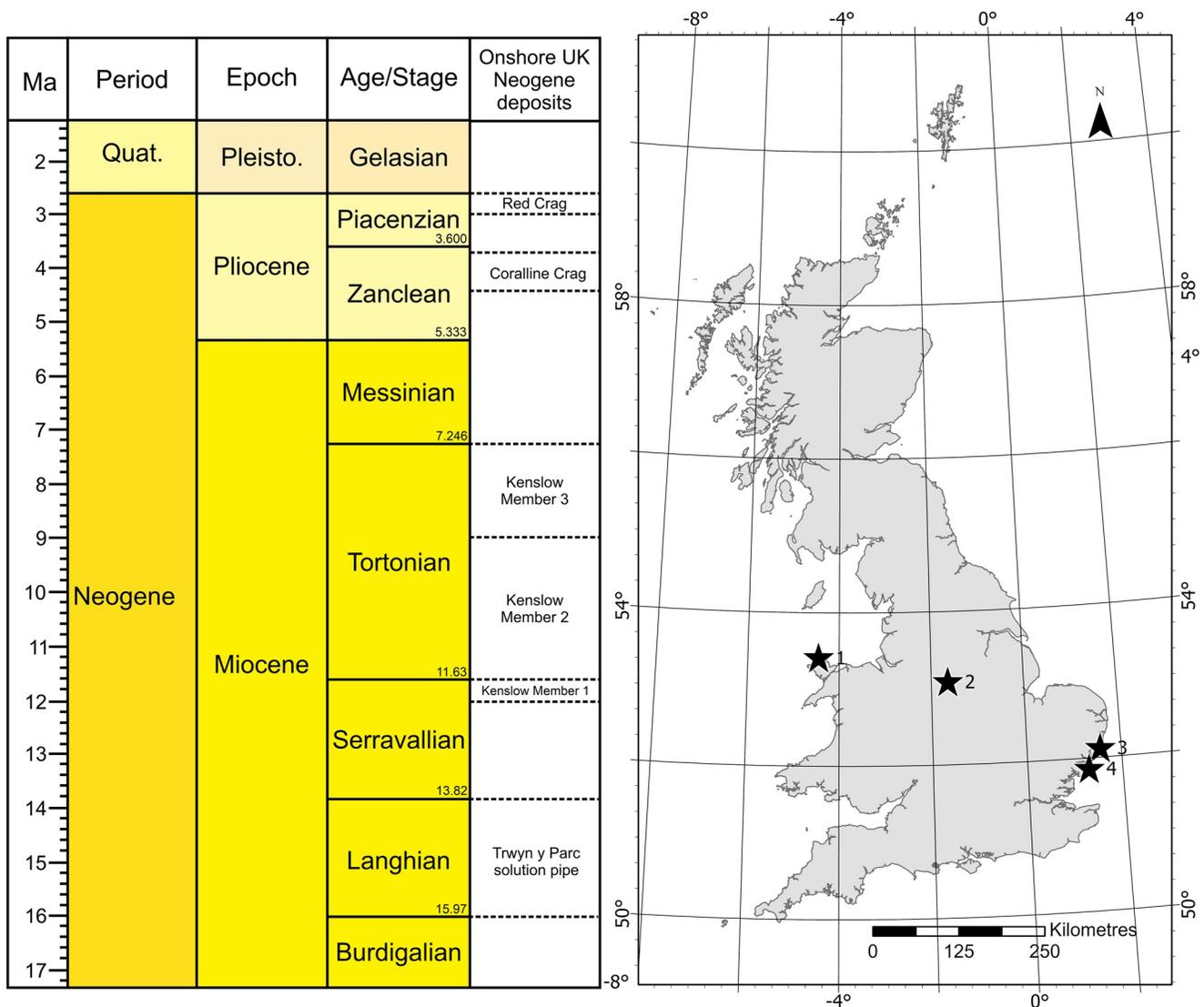
Figure 1. Stratigraphy of UK Neogene deposits and their geographical distribution. (1) Trwyn y Parc solution pipe fill (Pound & McCoy, 2021; Walsh et al., 1996); (2) Brassington Formation, Kenslow Member 1, 2 and 3 (Pound & Riding, 2016; Pound, Riding, et al., 2012); (3) Coralline Crag Formation, Ramsholt Member (King, 2016; Vignols et al., 2019); (4) Red Crag Formation at Walton-on-the-Naze (Head, 1998; King, 2016).

Changes in mean annual precipitation could not be interpreted due to the overlapping ranges reconstructed by the Co-existence Approach (Pound & Riding, 2016).

The climate of the latest Zanclean—earliest Piacenzian Coralline Crag Formation has been reconstructed based on the taxonomic composition of bivalve taxa and isotopic ($\delta^{18}O$) evidence of seasonal seafloor temperatures from serial ontogenetic sampling of bivalve shells (Vignols et al., 2019; Williams et al., 2009). Williams et al. (2009) indicated cool temperate winter (<10°C) and/or summer (<20°C) conditions. More recent $\delta^{18}O$ data are strongly consistent with cool temperate seafloor conditions (Vignols et al., 2019) with summer maximum surface temperature reconstructed c. 5°C above seafloor temperature. This is only slightly higher that at present (17°–19°C as opposed to 16°–17°C). Winter minimum surface temperature were reconstructed below 10°C and within the same range as at present (6°–7°C). The expanded surface temperature range compared to now was interpreted as possibly reflecting withdrawal of oceanic heat supply combined with higher global temperatures (Vignols et al., 2019). Otherwise, mollusks, ostracods, foraminifera and dinoflagellate cysts indicate a warm "Mediterranean" climate (Balson, 1999a, 1999b; Head, 1997; Wood et al., 1993). The Piacenzian-Gelasian Red Crag Formation probably contains multiple short intervals of time crossing the Pliocene—Pleistocene boundary that is

best exemplified by the contrasting paleoclimate reconstructions from Walton-on-the-Naze and Buckanay Farm outcrops (Head, 1998; Wood, 2012). At Walton-on-the-Naze (latest Piacenzian) the pollen and spore assemblages indicate a mild-to warm-temperate climate (Head, 1998). Conversely, the ostracod assemblage at Buckanay Farm (earliest Gelasian) is cryophilic and indicative of an early cold phase in the Pleistocene (Wood, 2012).

2. Materials and Methods

Three techniques have been applied to reconstruct terrestrial paleoclimates of the Neogene from the UK. The widely utilized Co-existence Approach is compared to two distinct statistical techniques: CREST(Climate REconstruction SofTware; Chevalier et al., 2014) and CRACLE (Climate Reconstruction using Coexistence Likelihood Estimation; Harbert & Baryiames, 2020; Harbert & Nixon, 2015). The aim is to better capture uncertainties in terrestrial climate reconstructions. Two different approaches were employed that provide an estimation of uncertainty. Taxa lists, palynomorph abundances and nearest living relatives, where possible, were extracted from the literature outlined below and used as the input for CREST, CRACLE and the Co-existence Approach.

2.1. Fossil Deposits Used

The Miocene paleoclimates of the UK are reconstructed for the Langhian — Tortonian. Whilst the Mochras Borehole may contain Aquitanian pollen assemblages towards the top of the Cenozoic sequence, this has not been recently confirmed and is in need of a re-study (Herbert-Smith, 1971). As there are no known onshore Burdigalian sediments in the UK, the oldest onshore Miocene deposits in the UK are from a complex of 15 solution pipes on the Isle of Anglesey in northwest Wales (Figure 1). The original pollen and spore taxa list of Walsh et al. (1996) was updated by Pound and McCoy (2021) who also applied the Co-existence Approach to reconstruct paleoclimate. This updated taxa list and the Co-existence Approach results are used in this study.

The Brassington Formation of Derbyshire and Staffordshire is the most extensive onshore Miocene sedimentary succession in the UK. It is a succession of sands, gravels and clays found in c. 60 karstic cavities distributed in the southern part of the Lower Carboniferous Peak Limestone Group outcrop of the Peak District. The uppermost Kenslow Member has a diachronous age of Serravallian to Tortonian depending on the outcrop (Pound & Riding, 2016). The palynoflora from the oldest sample (KM-1, Bees Nest Pit; Pound & Riding, 2016) represents a subtropical conifer-dominated forest of late Serravallian age (c. 12 Ma). The palynoflora of the younger samples KM-2 (Kenslow Top Pit, clay from wood fragment; Pound & Riding, 2016) and KM-3 (Kenslow Top Pit; Pound, Riding, et al., 2012) represent a subtropical mixed forest of early Tortonian (11.6–9 Ma) and late Tortonian age (9–7.3 Ma) respectively. Taxa lists and Co-existence Approach likelihood ranges were taken from Pound, Riding, et al. (2012) and Pound and Riding (2016). There are currently no known onshore Messinian fossiliferous sediments in the UK.

The paleoclimate of the Pliocene is based upon the Coralline Crag and Red Crag formations. The Coralline Crag Formation taxa lists come from the Ramsholt Member which is dated between 3.7 and 3.5 Ma (King, 2016) and 4.1–3.7 Ma based on dinoflagellate cyst records (De Schepper et al., 2008; Zanclean). The unit is composed of silty, shelly, bioturbated, glauconitic, fine to medium calcareous sand. The palynoflora represents a regionally dominant nearshore forest composed of inland taxa as well as those adapted to eutrophic or oligotrophic lowland mires (Andrew & West, 1977). Taxa lists were obtained from samples O33, O35, O36 and O38 of the original palynological analysis of the Ramsholt Member by Andrew and West (1977).

The Red Crag Formation taxa lists come from samples WC1-4 of Head (1998) from the Walton Crag at Walton-on-the-Naze. Samples WC1-3 come from the lowest 5 cm of a 0.5–1.5 m-thick horizontal layer of the Walton Crag that directly overlies the London Clay and are latest Piacenzian in age. This layer is weakly consolidated, consisting of greyish to buff-coloured, coarse, poorly sorted, shelly sands, indicative of bioturbation. Sample WC4 comes from a moderately calcareous, red-stained, silty lamina up to 1 cm thick occurring 2 m above the base of the Walton Crag (Head, 1998). A combination of pollen, dinoflagellate cysts and foraminifera all indicate a latest Piacenzian date (King, 2016), with the palynoflora of WC1-3 representing a mild-warm-temperature forest and WC4 signalling a stronger contribution from coastal swamp vegetation while maintaining mild- or warm-temperate conditions (Head, 1998).

Original taxa lists were used and following the recommendations of Utescher et al. (2014) relict taxa *Cathaya*, *Cryptomeria*, *Pinus sylvestris*, and *Sciadopitys* were removed before analysis. Full taxa lists and associated NLRs can be found in Data Set S1. Results including relic taxa can be found in Data Set S2. Modern climate values for Mean Annual Temperature (MAT), Mean Temperature of Warmest Month (MTWM), Mean Temperature of Coldest Month (MTCM), Mean Annual Precipitation (MAP) and precipitation seasonality were extracted from WorldClim 2.1 (Fick & Hijmans, 2017) and are presented as an average of the four locations. Full modern climatology for the four sites is presented in Table S2.

2.2. Reconstruction Technique Descriptions

CREST (Climate REconstruction SofTware) is a Bayesian approach that combines presence-only plant occurrence data with modern climatological data to estimate the conditional responses of pollen taxa to specific climate variables (Chevalier, 2019; Chevalier et al., 2014). The probabilistic nature of CREST produces reconstructions in the form of posterior distributions of probabilities that describe the likelihood of all climate values along the studied climate gradient, not just a single mean or optima associated with a standard error. The taxon-climate responses are defined as probability density functions (*pdfs*) When applied to pollen data a parametric *pdf* is first fitted to all the species belonging to the pollen type. The species *pdfs* are combined into a higher order pollen type *pdf*. A benefit of CREST over other reconstructions techniques is that *pdfs* can be multimodal, and depending on the climate variable being reconstructed, a normal or lognormal *pdf* can be fitted. As such, normal *pdfs* were used to reconstruct temperature variables while lognormal *pdfs* were used for precipitation variables. For more detail on the method, see Chevalier et al. (2014) and original documentation of the "CREST" R code is available with the package code (https://github.com/mchevalier2/crestr).

CRACLE (Climate Reconstruction Analysis using Coexistence Likelihood Estimation) derives the most likely climate for the combination of taxa identified using joint likelihood functions, based on modern distribution data (Harbert & Nixon, 2015). CRACLE generates two types of distribution to calculate this probability: a normal distribution for a parametric likelihood function (P-CRACLE) and a non-parametric likelihood function (N-CRACLE). Furthermore, the N-CRACLE method makes no assumption about the shape of the distribution in climatic space, other than that the distribution is continuous and smooth. Therefore, it is likely more suited to assemblages containing relic taxa, taxa for which responses to bioclimate variables are unclear such as in deeper time reconstructions. Therefore, in this study we focus on the results of N-CRACLE to accommodate for this. For more detail on the method, see Harbert and Nixon (2015) and the "cRacle" package is explained in detail in Harbert and Baryiames (2020). Original documentation of the "cRacle" R code is available with the package code (https://github.com/rsh249/cRacle).

The Co-existence Approach (Mosbrugger & Utescher, 1997; Utescher et al., 2014) is a non-probabilistic approach which calculates climate estimates based on the total overlap of climate tolerances of the nearest living relatives (NLRs) of the flora. For each fossil taxon, a NLR is identified, and its modern distribution is compiled. For each climate variable analyzed, a coexistence interval is determined based on the maximum number of NLRs that can coexist within a climate range. This is considered to be the best description of the paleoclimate in which the given fossil flora lived. CREST and CRACLE significantly improve on the error from previous paleovegetation methods while integrating community data to help mitigate the effects of mixed floral assemblages and address some other methodological issues of the Co-existence Approach (Grimm & Potts, 2016). Co-existence Approach reconstructions for Trwyn y Parc and the Brassington Formation come from Pound and McCoy (2021) and Pound and Riding (2016) respectively. Co-existence Approach reconstructions for the Coralline Crag and Red Crag formations were determined for this study.

CREST and CRACLE differ from other *pdf*-based techniques in how they process data. They differ from the Co-existence Approach in that they use the GBIF (Global Biodiversity Information Facility; GBIF, 2021) database observations but also WorldClim as inputs for the 19 climate variables used by BIOCLIM (http://www.worldclim.org/bioclim). Meanwhile, the Co-existence Approach uses the Palaeoflora database, meaning the input data for the three techniques is different (Grimm & Potts, 2016; Utescher et al., 2014). Five climate variables were assessed in detail: Mean Annual Temperature (MAT), Mean Temperature of Warmest Quarter (MTWQ), Mean Temperature of Coldest Quarter (MTCQ), Mean Annual Precipitation (MAP) and Precipitation Seasonality (CoV × 100). The Co-existence Approach does not reconstruct MTMQ, MTCQ or precipitation seasonality. Instead, the Co-existence Approach reconstructions for Warmest Month Mean Temperature (WMMT) and
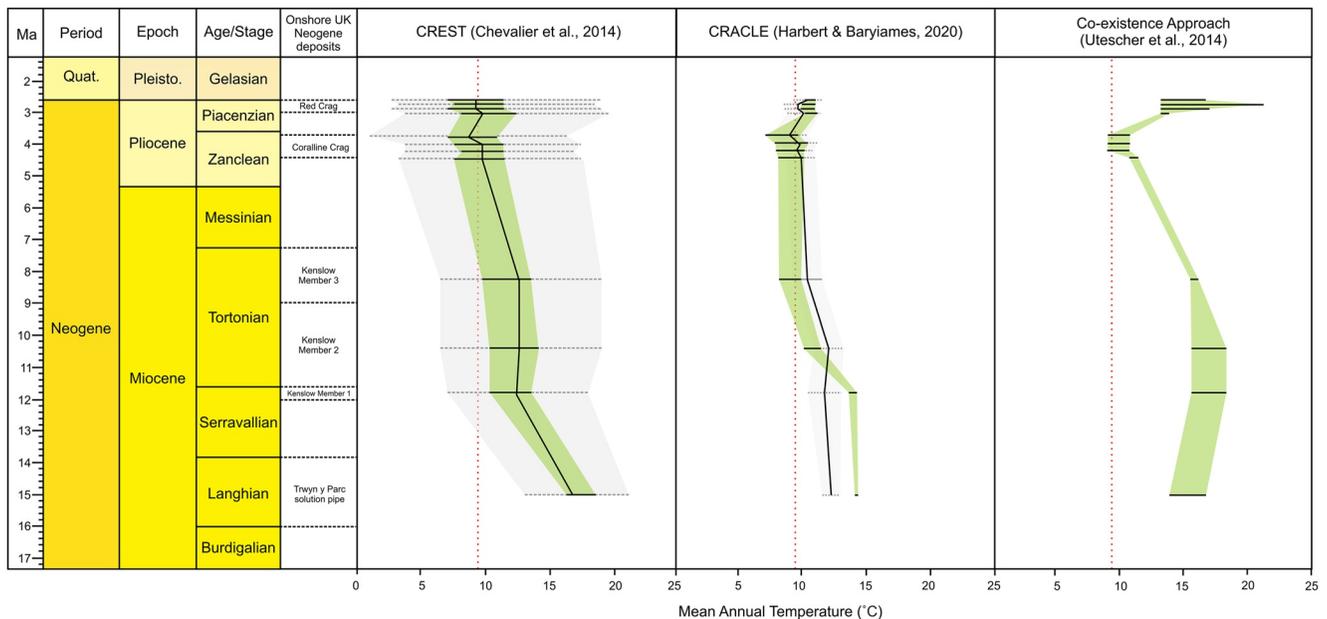
Figure 2. Mean Annual Temperature (MAT) reconstructed by CREST, CRACLE and the Co-existence Approach. CREST: 0.5 uncertainties highlighted in green, 0.95 (2-σ) uncertainties in grey, optima represented by a solid black line. CRACLE: N-CRACLE 0.95 (2-σ) uncertainties in green, P-CRACLE 0.95 (2-σ) uncertainties in grey, mean represented by a solid black line. Co-existence Approach: equal likelihood range in green. Modern MAT (9.5°C) as a dotted red line.

Coldest Month Mean Temperature (CMMT) were used as comparisons for MTMQ and MTCQ respectively. The proportion of rainfall falling in the wettest months of the year (RMPwet [%]) was used as a proxy for precipitation seasonality following the methodology of Jaques et al. (2011) and Utescher et al. (2015).

The CREST R-code output provides 0.5 and 0.95 (2-σ) uncertainties as well as an optimum and mean for each climate variable. The output for the CRACLE R-code provides the results for both parametric and non-parametric joint likelihoods (P-CRACLE and N-CRACLE) with 0.95 (2-σ) uncertainties on the likelihood distribution as well as a mean. It should be noted that the mean is based on P-CRACLE. Therefore, the CRACLE mean can lie outside the 0.95 uncertainties for N-CRACLE. The Co-existence Approach generates a minimum and maximum likelihood which together comprise the coexistence interval. Sample R-code for both CREST and CRACLE are provided in the Supporting Information.

3. Results

Climate change in the UK from the Middle Miocene to the latest Piacenzian is characterized by a decrease in MAT (Figure 2), MTWQ (Figure 3) and MTCQ (Figure 4), and during the later Miocene, followed by an increase during the late Pliocene (Piacenzian). MAP decreases throughout the Miocene, increasing into the Pliocene before declining at the Piacenzian–Gelasian boundary (Figure 5). Precipitation seasonality declines throughout the Miocene, increasing throughout the Pliocene, finally declining in the Piacenzian (Figure 6). The reconstructions for the three techniques can be found in Table S1.

3.1. Mean Annual Temperature (MAT)

CREST reconstructs a decline in MAT (Mean Annual Temperature) from 16.9°C (13.1°–1.2°C) to 12.5°C (7.1°–17.9°C) from the Langhian to the late Serravallian and remains consistent at 12.6°C (6.6°–19.0°C) during the early Tortonian and late Tortonian. CREST reconstructs a c. 2.8°C cooling from 12.6°C (6.6°–19.0°C) to 9.8°C (3.3°–17.4°C) from the Tortonian to the Zanclean, remaining relatively constant throughout the Zanclean before declining to 8.7°C (1.1°–16.3°C) in the youngest sample from the Coralline Crag Formation (O33). CREST reconstructs a slight increase in MAT of 1.1°C from 8.7°C (1.1°–16.3°C) to 9.8°C (3.8°–19.6°C) from the Zanclean to the Piacenzian. During the Piacenzian there is an overall minor decline in MAT of 0.5°C from 9.8°C (3.8°–19.6°C) to 9.3°C (2.8°–19.0°C) in the youngest two Piacenzian samples (WC3 and WC4).
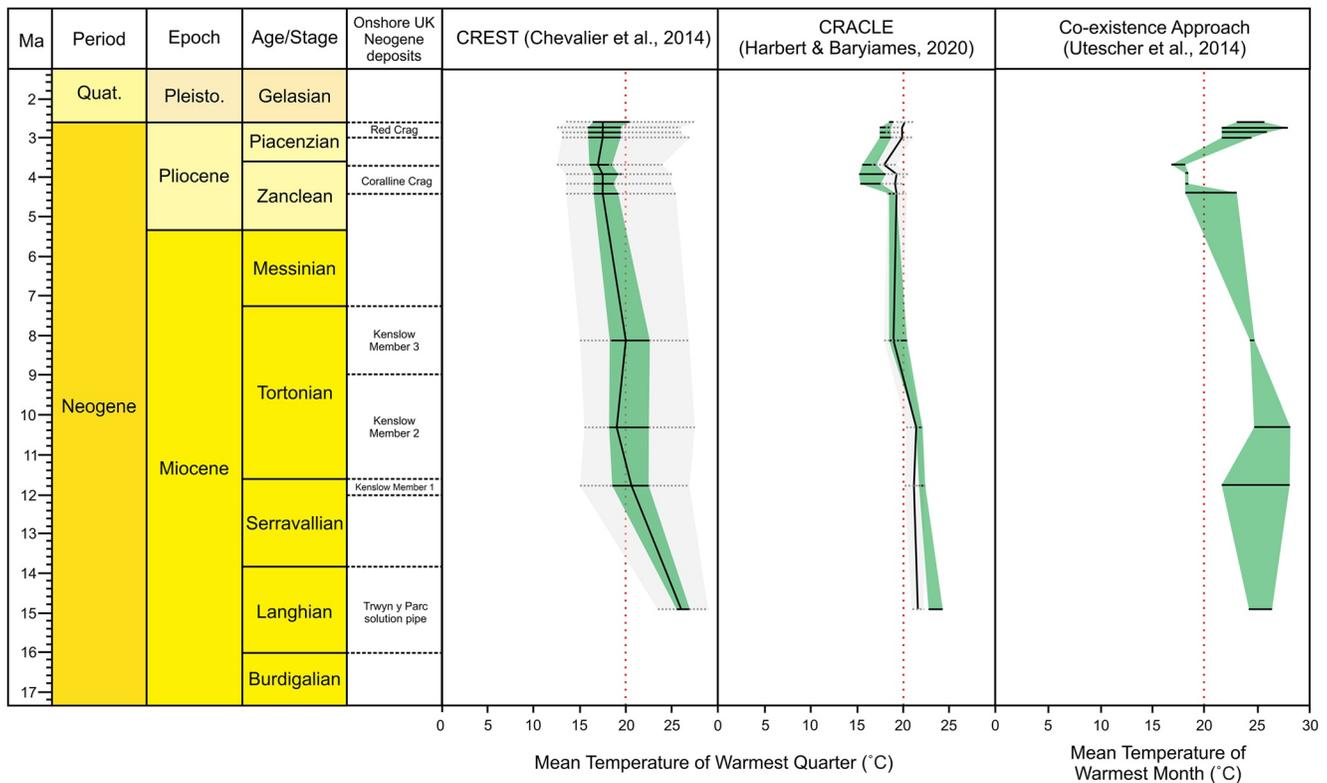
Figure 3. Mean Temperature of Warmest Quarter (MTWQ) reconstructed by CREST and CRACLE compared to Mean Temperature of the Warmest Month (MTWM) by the Co-existence Approach. CREST: 0.5 uncertainties in dark green, 0.95 (2-σ) uncertainties in grey, optima represented by solid black line. CRACLE: N-CRACLE 0.95 (2-σ) uncertainties in dark green, P-CRACLE 0.95 (2-σ) uncertainties in grey, mean represented by a solid black line. Co-existence Approach: equal likelihood range in light blue. Modern MTWM (20.°C) as a dotted red line.

N-CRACLE reconstructs a decline in MAT from 14°C ± 0.1°C in the Langhian to 13.7°C ± 0.3°C in the late Serravallian followed by a 1.6°C decline in MAT through the Tortonian from 10.5°C ± 0.5 to 8.9°C ± 0.9°C. N-CRACLE reconstructs no change in MAT from the Tortonian to the Zanclean, with a slight decline in MAT across the Zanclean from 8.9°C ± 0.9°C to 8.2°C ± 1.1°C. N-CRACLE reconstructs a 2.2°C increase in MAT 8.2°C ± 1.1°C to 10.5°C ± 0.5°C from the Zanclean to the Piacenzian, and a very minor decline (>0.5°C) in MAT from 10.5°C ± 0.5°C in WC1 to 10.3°C ± 0.3°C in WC3, before increasing to 10.4°C ± 0.4°C towards the Piacenzian–Gelasian boundary (WC4).

P-CRACLE reconstructs a cooler Langhian MAT of 12.1°C ± 0.7°C declining to 11.5°C ± 0.13°C in the late Serravallian. During the Tortonian, P-CRACLE reconstructs a slightly warmer MAT of 11.8°C ± 1.2°C in the early Tortonian which declines to 10.1°C ± 1.1°C during the late Tortonian. P-CRACLE reconstructs a decline in MAT into the Pliocene with temperatures being slightly warmer than N-CRACLE throughout the Zanclean, with a decline from 9.7°C ± 1.2°C (O38) to 8.8°C ± 1.4°C (O33). P-CRACLE MAT is cooler in the Piacenzian than N-CRACLE but slightly higher than Zanclean estimates. MAT increases c. 1. °C to 9.9°C ± 1.3°C from the Zanclean to the Piacenzian but declines in WC2 and WC3 to 9.4°C ± 1.0°C, before rising to 10.2°C ± 1.1°C in the final Piacenzian sample (WC4).

The Co-existence Approach reconstructs an increase in MAT range from the Langhian to the late Serravallian from 16.9°–18.1°C to 15.7°–18.4°C followed by a decline in MAT from 15.7°–18.4°C to 15.6°–16.2°C during the Tortonian. The Co-existence Approach reconstructs a c. 5. °C decline in MAT from the Tortonian to Zanclean from 15.6°–16.2°C to 10.8°–11.5°C, falling to 9.1°–10.8°C throughout the Coralline Crag Formation. MAT is reconstructed to increase from the Zanclean to the Piacenzian from 9.1°–10.8°C to 13.3°–13.8°C. Throughout the Piacenzian MATmax increases from 13.8°C to 21.3°C while MATmin remains constant at 13.3°C. A decline in MATmax is reconstructed for the last Piacenzian sample (WC4) with no change in MATmin 13.3°–16.8°C.
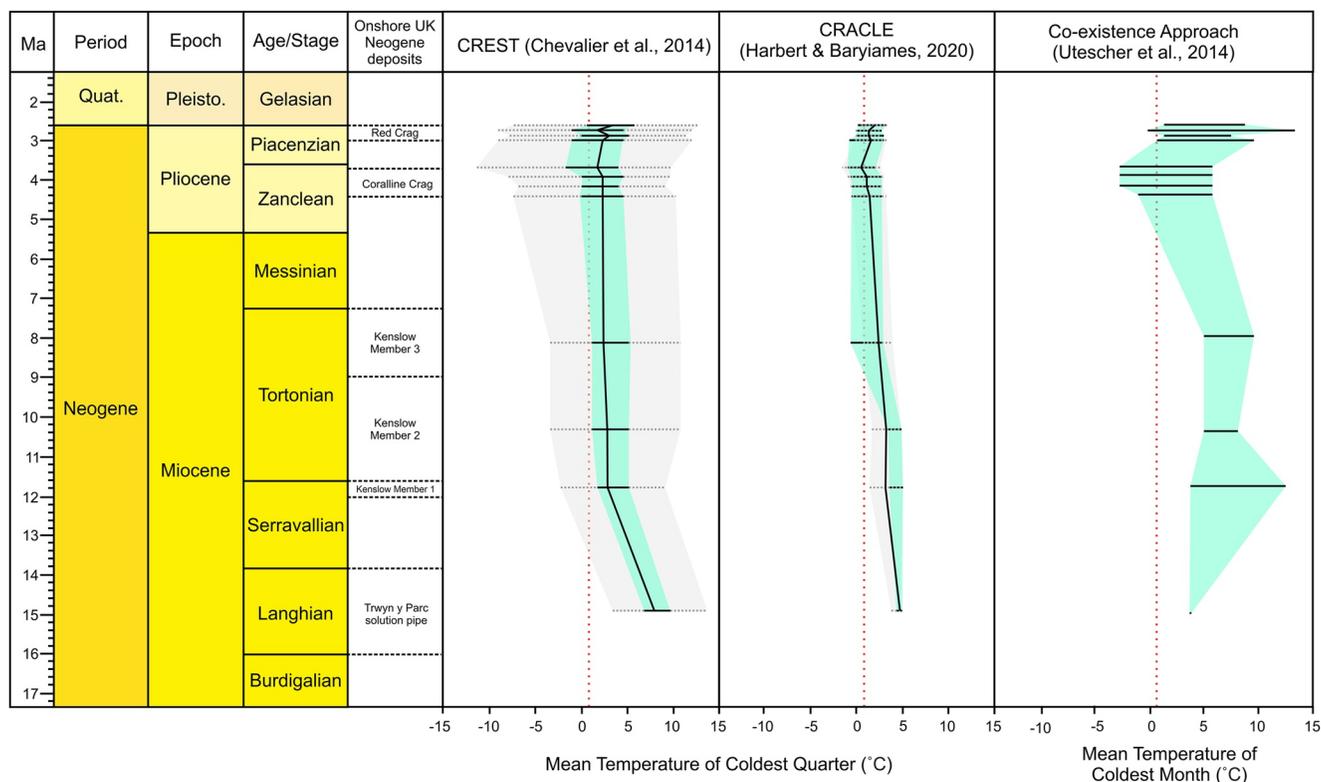
Figure 4. Mean Temperature of Coldest Quarter (MTCQ) reconstruction using CREST, CRACLE compared to Mean Temperature of the Coldest Month (MTCM) by the Co-existence Approach. CREST: 0.5 uncertainties in aqua, 0.95 (2-σ) uncertainties in grey, optima represented by a solid black line. CRACLE: N-CRACLE 0.95 (2-σ) uncertainties interval in aqua, P-CRACLE 0.95 (2-σ) uncertainties in grey, mean represented by a solid black line. Co-existence Approach: equal likelihood range in dark blue. Modern mean temperature of coldest month (1.4°C) as a dotted red line.
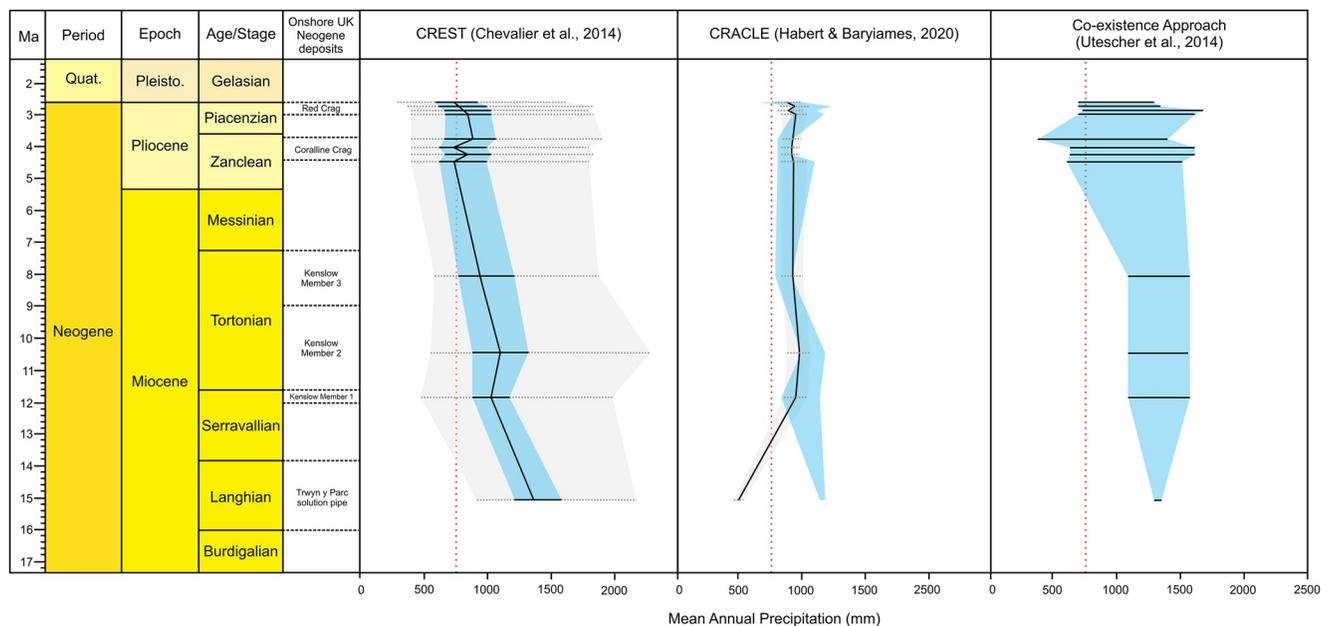
Figure 5. Mean Annual Precipitation (MAP) reconstructed by CREST, CRACLE and the Co-existence Approach. CREST: 0.5 uncertainties in blue, 0.95 (2-σ) uncertainties in grey, optima represented by a solid black line. CRACLE: N-CRACLE 0.95 (2-σ) uncertainties in blue, P-CRACLE 0.95 (2-σ) uncertainties in blue, mean represented by a solid black line. Co-existence Approach: equal likelihood range in blue. Modern MAP (747 mm) as a dotted red line.

Figure 6. Precipitation Seasonality (CoV × 100) reconstructed by CREST, CRACLE compared to RMPwet (%) by the Co-existence Approach. CREST: 0.5 uncertainties in orange, 0.95 (2-σ) uncertainties in grey, optima represented by a solid black line. CRACLE: N-CRA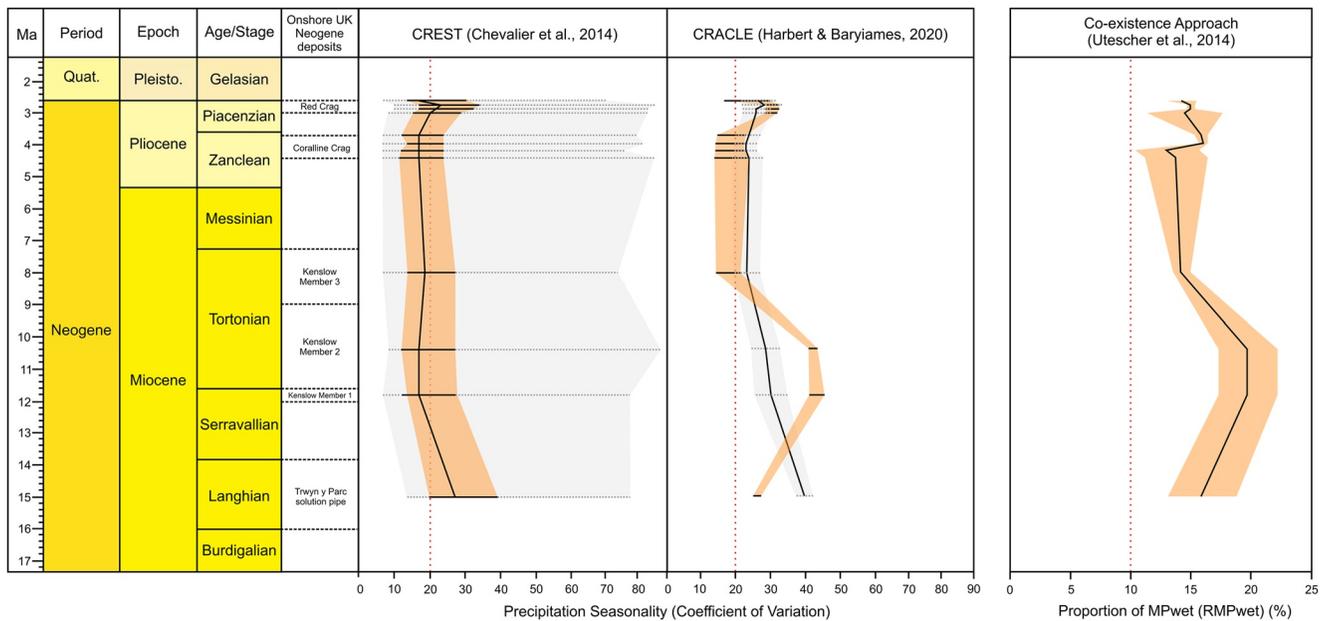CLE 0.95 (2-σ) uncertainties in orange, P-CRACLE 0.95 (2-σ) uncertainties in grey, mean represented by a solid black line. Modern precipitation seasonality as a dotted red line (20). Co-existence Aproach: proportion of MPwet (RMPwet) (%), mean represented by a solid black line. Modern RMPwet (10%) as a red dotted line.

3.2. Warm Month Temperatures

CREST reconstructs a drop in MTWQ (Mean Temperature of Warmest Quarter) from 5.4°C (22.9°–28.3°C) to 20.6°C (14.8°–26.4°C) from the Langhian to the Serravallian. MTWQ declines from the Serravallian through the Tortonian by c. 1.5°C to 18.6°C (15.3°–26.8°C), before increasing to 19.6°C (14.8–26.4°C) during the late Tortonian. MTWQ is reconstructed c. 2°C cooler in the Zanclean compared to the late Tortonian and MTWQ declines from 17.2°C (13.3°–24.9°C) in O38 to 16.7°C (12.4°–23.5°C). MTWQ remains constant throughout the Piacenzian at 17.2°C but shifts in the confidence interval from 12.9°–25.4°C to 13.3°–26.8°C in the youngest sample from the Red Crag Formation, suggestive of warming.

N-CRACLE reconstructs a 2.3°C in MTWQ from 23.5°C ± 0.8°C to 21.9°C ± 0.3°C from the Langhian to the late Serravallian followed by a 2.5°C decline in MTWQ to 19.4°C ± 1.0°C by the late Tortonian. MTWQ decreases marginally (c. 0.5°C) from 19.4°C ± 1.0°C to 18.8°C ± 0.4°C from the late Tortonian to the Zanclean before dropping to 16.3°C ± 0.8°C in the youngest sample from the Coralline Crag Formation. MTWQ is then reconstructed to increase 1.8°C to 18.0°C ± 0.5°C during the Piacenzian, before decreasing to 17.9°C ± 0.4°C in samples WC2 and WC3 before finally increasing to 18.6°C ± 0.3°C in youngest sample from the Red Crag Formation (WC4).

P-CRACLE reconstructions for warm month temperatures during the Middle Miocene are cooler than N-CRACLE. MTWQ is consistent from the Langhian to Tortonian at 21.5°C ± 0.6°C in the Langhian, 21.1°C ± 1.1°C in the late Serravallian, and 21.3°C ± 1. °C in the early Tortonian. MTWQ then falls in the late Tortonian to 18.9°C ± 1.0°C which overlaps with the N-CRACLE reconstruction. P-CRACLE MTWQ is slightly higher than the N-CRACLE reconstruction in the Pliocene but is cooler than the P-CRACLE Miocene reconstruction. From the late Tortonian to the Zanclean MTWQ increases by c. 0.5°C to 19.3°C ± 1. °C (O38), before falling to 18.8°C ± 1. °C (O36), rising again to 19.4°C ± 1.2°C (O35), before falling to a Neogene low of 17.9°C ± 1.3°C (O33). MTWQ increases into the Piacenzian by c. 2. °C to 19.8°C ± 1.1°C (WC1). P-CRACLE reconstructs a lower MTWQ in samples WC2 and WC3 of 18.9°C ± 0.8°C before a final increase in the youngest sample from the Red Crag Formation of c. 1.5°C to 20.1°C ± 0.9°C.

The Co-existence Approach reconstructs an increase in MTWM (Mean Temperature of Warmest Month) from 24.3°–26.5°C to 21.6°–28.1°C from the Langhian to the late Serravallian. MTWM increases from the Serravallian

to the early Tortonian to 24.7–28.1°C before decreasing to 24.7°–24.3°C in the late Tortonian. There is a drop from 24.3°–24.7°C to 18.1°–23.°C in MTWM from the Tortonian to the Zanclean and MTWMmax steadily decreases from 23.°C to 16.8°C. The Co-existence Approach reconstructs a decline in MTWM from the late Tortonian into the Zanclean from 24.3-24.7°C to 18.1°–23.°C. During the Zanclean MTWMmin declines from 23.°C to 16.8°C. From the Zanclean to the Piacenzian MTWM increases from 16.8°–18.1°C to 21.6–24.4°C. During the Piacenzian MTWM increases to 21.6°–27.9°C. For the final Piacenzian sample (WC4) the likelihood range shrinks as the maximum bound decreases to 25.7°C but the minimum bound increases to 23.°C suggesting an overall increase in MTWM.

3.3. Cold Month Temperatures

CREST reconstructs a decline in MTCQ (Mean Temperature of Coldest Quarter) from 8.8°C (4.1°–14.7°C) to 3.5°C (−1.9° to 9.9°C) from the Langhian to the late Serravallian and only declines slightly through the Tortonian from 3.5°C (−1.9° to 9.9°C) to 2.9°C (−3.1° to 11.2°C). CREST does not reconstruct any change in MTCQ from the Tortonian to the Zanclean until the youngest sample O33 to 2.3°C (−11.4° to 10.6°C). MTCQ increases by 1.2°C from the Zanclean to the Piacenzian from 2.3°C (−11.3° to 10.6°C) to 3.5°C (−8.9° to 12.4°C) in WC2. MTCQ declines to 2.3°C (−8.9° to 12.9°C) in WC3 before increasing 1.8°C to 4.1°C (−7.2° to 13.5°C) in the youngest sample from the Red Crag Formation (WC4).

N-CRACLE reconstructs a decline in MTCQ from the Langhian to the late Serravallian from 4.6°C ± 0.3°C to 4.3°C ± 0.8°C, continuing to decline throughout the Tortonian from 4.1°C ± 0.7°C during the early Tortonian to 1.1°C ± 1.8°C during the late Tortonian. MTCQ continues to decline from the Tortonian to the Zanclean to 1.0°C ± 1.6°C and continues to decline throughout the Zanclean samples to 0.5°C ± 1.5°C in the final sample from the Coralline Crag Formation (O33). N-CRACLE reconstructs a rise of 0.6°C in MTCQ into the Piacenzian to 1.1°C ± 1.9°C (WC1), followed by a rise to 1.3°C ± 1.4°C in samples WC2 and WC3. A MTCQ of 1.6°C ± 1.5°C is reconstructed for the youngest sample from the Red Crag Formation (WC4).

P-CRACLE reconstructs a decline in MTCQ of over 1.5°C from the Langhian to the late Serravallian from 4.7°C ± 1.°C to 3.1°C ± 1.7°C. MTCQ remains constant into the early Tortonian at 3.2°C ± 1.6°C but falls into the late Tortonian to 2.3°C ± 1.5°C. Cold month temperatures continue to decline into the Zanclean where P-CRACLE reconstructs a 1°C in MTCQ to 1.3°C ± 1.8°C (O38). Cold month temperatures decline throughout the Zanclean, dropping to 0.5°C ± 2.°C in the youngest sample from the Coralline Crag Formation (O33). Piacenzian cold month temperatures are warmer than in the Zanclean with a c. 1.5°C increase in MTCQ to 1.6°C ± 1.8°C in WC1. Cold month temperatures continue to increase throughout the Piacenzian to 1.9°C ± 1.4°C in the youngest sample from the Red Crag Formation.

The Co-existence Approach reconstructs an increase in MTCM (Mean Temperature of Coldest Month) from 3.7° to 3.8°C in the Langhian to a considerably larger range for the late Serravallian of 3.8°–12.5°C, yet the MTCMmin remains essentially constant. A warmer MTCM during the early and late Tortonian (5.0°–8.1°C and 5°–9.6°C respectively) than during the late Serravallian. A considerable decline in MTCM is reconstructed from the Tortonian to the Zanclean from 5.0–9.6°C to −1.°–5.8°C, continuing to decline through the Zanclean to −2.7° to 5.8°C. The Co-existence Approach reconstructs a considerable increase in MTCM minimum to above freezing from the Zanclean to the Piacenzian from −2.7°–5.8°C to 0.7°–9.6°C. In WC2 MTCM increases to 1.4°–7.5°C before decreasing and expanding in range to −0.1°–13.3°C in WC3. In the latest Piacenzian (WC4) MTCM is reconstructed higher at 1.4°–8.8°C.

3.4. Mean Annual Precipitation (MAP)

CREST reconstructs a steady decline in MAP (Mean Annual Precipitation) from a high of 1,351 mm (919–2,170 mm) in the Langhian, to 1,029 mm (478–1,986 mm) in the late Serravallian, followed by a slight increase to 12,103 mm (552–2,280 mm) in the early Tortonian and a decline to 956 mm (588–1,875 mm) in the late Tortonian. From the Tortonian to the Zanclean CREST reconstructs a decline in MAP from 956 mm (588–1,875 mm) to 846 mm (368–1,839 mm). During the Zanclean MAP continues to decline to 735 mm (294–1,618 mm) throughout the Coralline Crag Formation. CREST reconstructs a consistent MAP across the Zanclean and Piacenzian, before increasing to 846 mm (405–1,839 mm) in WC2 and declining to 736 mm (405–1,802 mm) in WC3. MAP increases to 883 mm (405–1,912 mm) in WC4.

N-CRACLE reconstructs a Langhian MAP of 1,134 mm ± 19 mm. MAP decreases to 955 mm ± 150 mm during the Serravallian, then increases to 1,061 mm ± 102 mm in the early Tortonian, followed by a decrease to 819 mm ± 63 mm during the late Tortonian. N-CRACLE reconstructs a 200 mm increase in MAP from the Tortonian to the Zanclean to 1,018 mm ± 126 mm. During the Zanclean however, MAP varies. From O38 to O36 MAP declines to 984 mm ± 102 mm, increasing to 1,052 mm ± 141 mm in O35, finally declining to 732 mm ± 111 mm in the youngest sample from the Coralline Crag Formation. N-CRACLE reconstructs an increase in MAP from the Zanclean to Piacenzian of c. 200 to 921 mm ± 145 mm (WC1). During the Piacenzian MAP decreases c. 100 to 824 mm ± 48 mm (WC2 and WC3), before increasing slightly to 838 mm ± 63 mm in the youngest sample from the Red Crag Formation (WC4).

In general, P-CRACLE reconstructs lower MAPs than N-CRACLE with mean MAP never exceeding 1,000 mm. P-CRACLE reconstructs a very low MAP for the Langhian at 466 mm ± 38 mm. MAP is reconstructed to almost double into the late Serravallian to 916 mm ± 92 mm with a further increase into the early Tortonian to 946 mm ± 92 mm, followed by a decrease to 890 mm ± 80 mm in the late Tortonian. MAP increases slightly into the Zanclean to 907 mm ± 100 mm (O38) before dropping >100 to 874 mm ± 95 mm (O36). MAP then increases to 911 mm ± 117 mm (O35) before dropping again to 849 mm ± 95 mm. MAP increases by 50 mm into the Piacenzian to 900 mm ± 98 mm, following which MAP declines slightly to 880 mm ± 70 mm with a minimal increase in the youngest Piacenzian sample 888 mm ± 71 mm.

The Co-existence Approach reconstructs a decline in MAPmin and increase in MAPmax from the Langhian to the late Serravallian from 1,300–1,356 to 1.096–1,577 mm. MAP remains relatively constant during the early Tortonian (1,096–1.652 mm) and late Tortonian (1,096–1,577 mm). The Co-existence Approach reconstructs a considerable decline in MAPmin from the Tortonian to the Zanclean from 1098-1,577 mm to 619–1,520 mm (O38) while the MAPmax remains relatively constant. MAPmin then increases to 641–1,613 mm (O36, O35), before declining to 389–1,400 mm (O33). The Co-existence Approach reconstructs an increase in MAP from the Zanclean to the Piacenzian, from 389-1,400 mm to 703–1,613 mm. MAP during the Piacenzian declines, increases in WC2 to 735–1,347 mm but then MAPmin declines while MAPmax increases to 703–1,682 mm again. In the final sample WC4, MAPmin remains constant while MAPmax decreases considerably to 1,298 mm.

3.5. Precipitation Seasonality

CREST reconstructs a marked decrease in precipitation seasonality (CoV × 100) from the Langhian to late Serravallian from 27.3 (13.7–76.9) to 17.1 (6.8–76.8). Seasonality increases slightly into the early Tortonian to 17.1 (8.5–85.4) and increases again into the late Tortonian to 18.8 (6.8–73.5). CREST reconstructs a slight decline in precipitation seasonality from the Tortonian to the Zanclean from 18.8 (6.8–73.5) to 17.1 (6.8–83.7) in O38. Seasonality remains constant throughout the Zanclean, but the uncertainties gradually decrease, with some variation, to 11.9–78.6 in O33. Seasonality then increases into the Piacenzian to 20.5 (8.5–82.0) and increases throughout the Piacenzian to sample WC3 to 23.9 (10.3–83.7), before falling to 17.1 (6.8–70.1) in sample WC4.

N-CRACLE reconstructs an increase in precipitation seasonality from the Langhian to late Serravallian from 25.1 ± 1.2 to 42.2 ± 2.2. Precipitation seasonality declines slightly to 41.1 ± 1.3 in the early Tortonian and declines considerably in the late Tortonian to 17.0 ± 3.4. N-CRACLE reconstructs a similar precipitation seasonality in the Zanclean as for the late Tortonian. Precipitation seasonality is relatively constant during the Zanclean, with a seasonality of 17.7 ± 4.7 in O38, 17.3 ± 4.1 in O36 and O35, and 17.9 ± 4.8 in O33. Precipitation seasonality increases into the Piacenzian, rising to 29.3 ± 1.5 in WC1, continuing to rise through to WC3 to 30.1 ± 2.0, before falling to 22.3 ± 6.5 in the youngest sample from the Red Crag Formation (WC4).

P-CRACLE reconstructions of Miocene precipitation seasonality differ greatly from N-CRACLE. P-CRACLE reconstructs a higher precipitation seasonality in the Langhian of 38.7 ± 2.4, followed by a decline to 29.1 ± 4.6 in the late Serravallian. Precipitation seasonality continues to fall throughout the Miocene to 27.5 ± 4.1 in the early Tortonian to 22.1 ± 3.9 in the late Tortonian, were P-CRACLE estimates are higher than N-CRACLE estimates. Zanclean P-CRACLE precipitation seasonality is reconstructed very similar to the late Miocene and overlaps with the N-CRACLE reconstruction. Precipitation seasonality falls slightly within the Coralline Crag Formation from 22.4 ± 4.4 in O38 to 21.9 ± 3.1 in O35, before rising to 22.7 ± 3.3 in the youngest sample from the Coralline Crag Formation (O33). Piacenzian P-CRACLE precipitation seasonality is lower than the

N-CRACLE reconstruction but increases into the Piacenzian to 24.9 ± 4.2 (WC1), rising to 27.1 ± 5.1 in WC3, before declining to 25.5 ± 4.9 in the youngest sample from the Red Crag Formation (WC4).

The Co-existence Approach reconstructs RMPwet estimates, a measure of precipitation seasonality, of 15.9% (13.1%–18.7%) in the Langhian, increasing to 19.7% (17.3%–19.7%) during the late Serravallian and early Tortonian. RMPwet falls to 14.2% (13.5%–15.0%) in the late Tortonian. RMPwet continues to decline into the Zanclean, falling to 13.0% (11.2%–16.4%) in the lower part of Coralline Crag Formation (sample O36), rising to 16.1% (15.8%–16.4%) in the upper part (sample O35). From the Zanclean to the Piacenzian RMPwet falls to 14.5% (11.4%–17.6%; sample WC1) but is interrupted by a slight increase to 15.0% (14.6%–15.3%; samples WC2 and WC3) before falling to 14.2% (12.9%–15.4%) in the youngest sample from the Red Crag Formation (WC4).

4. Discussion

The three reconstruction techniques all show an overall trend of decreasing MAT and MAP throughout the Miocene and Pliocene in agreement with previous European terrestrial reconstructions (Mosbrugger et al., 2005; Utescher et al., 2015). In the first section of the discussion the climatic development of the UK is presented and compared to previous studies from northwest Europe and the North Atlantic. In the following section, the differences between techniques will be briefly discussed.

4.1. Climate Development of the UK

The three models show the Langhian from Trwyn y Parc to be the warmest interval of the UK Neogene (Figure 2). Although considered to be post-MCO in age (Pound & McCoy, 2021), the Trwyn y Parc assemblage still comes from a warm-interval of the Langhian before the major cooling step at Mi-3b identified from the nearby Porcupine Basin in the Western Approaches of the Atlantic Ocean and the Roer Valley Graben from the Netherlands (Donders et al., 2009; Quaijtaal et al., 2014). The reconstructed MAT by both CREST and CRACLE are comparable to the continental records from Germany that show a Middle Miocene MAT of c. 16°–21°C (Mosbrugger et al., 2005; Utescher et al., 2015). The reconstructed differences with present-day MAT are also consistent with multi-model mean surface temperature differences for northwest Europe at CO_2 values above 560 ppmv (Burls et al., 2021). Although not directly comparable, the winter temperatures reconstructed by CREST (MTCQ compared to MTCM for the Co-existence Approach) are on the colder end of the Co-existence Approach ranges reconstructed for the Lower Rhine and Weisselster basins (Utescher et al., 2015). However, both CREST and CRACLE reconstruct warmer winter temperatures than the Co-existence Approach for Trwyn y Parc: 8.8°C (4.1–14.7°C, 2-σ) by CREST, 4.5°C ± 0.3°C (2-σ) by N-CRACLE, and 3.7°–3.8°C by the Co-existence Approach (Figure 4). Summer temperature estimates for Trwyn y Parc by CREST 25.4°C (23.°–28.3°C, 2-σ; CREST), 23.5°C ± 0.55°C (N-CRACLE) and 24.3°–26.5°C (Co-existence Approach) fall within the range of North Atlantic Sea Surface Temperature (SST) reconstructions from ODP Site 982 from TEX_{86} and $U^{K'}_{37}$ of c. 22–26°C during the later Langhian (Super et al., 2020) and GDGT (glycerol dialkyl glycerol tetraethers) based reconstructions from the Roer Valley Graben (Donders et al., 2009). Both CREST and N-CRACLE reconstruct comparable MAP to the Co-existence Approach reconstructions from the Lower Rhine and Weisselster basins (Utescher et al., 2015). Both Trwyn y Parc and the reconstructions from Germany are above those based upon herpetological data from southwest Europe and Central-Eastern Europe around the Paratethys (Böhme et al., 2011) suggestive of a northwest to southeast precipitation gradient during the Langhian.

A cooling is reconstructed to have occurred between the Langhian of Trwyn y Parc and the Serravallian of the Brassington Formation of up to 4.4°C (Figure 2) consistent with global cooling during the Middle Miocene Climate Transition (Steinthorsdottir et al., 2021). However, the reconstructions by CREST and P-CRACLE of KM-1 from the Brassington Formation are cooler than those of the Lower Rhine and Weisselster basins (Utescher et al., 2015). The same is true for summer and winter reconstructions that remain constant in the Lower Rhine and Weisselster basins throughout the MCO and Middle Miocene Climate Transition (Utescher et al., 2015). CREST based reconstructions from the UK show a 4.8°C drop in summer temperatures (Figure 3) and a 5.3°C decrease in winter temperature (Figure 4). Whereas N-CRACLE shows smaller decreases of 0.3°C and 1.6°C for summer and winter, respectively (Figures 3 and 4). SST reconstructions from ODP Site 982 and GDGT reconstructions from the Roer Valley Graben show a ca. 4°C decrease through the MMCT, whilst dinoflagellate cyst-based reconstructions from Porcupine Basin also show a pronounced cooling at Mi-4 (Donders et al., 2009; Quaijtaal

et al., 2014; Super et al., 2020). A substantial cooling of ca. 17°C is reflected in recent Central European soil carbonate records (14.48–14.13 Ma; Methner et al., 2020), which is much larger than the temperature change known from deep-sea records (Holbourn et al., 2015; Lear et al., 2015; Levy et al., 2016; Shevenell et al., 2008; Super et al., 2018), other terrestrial studies which reconstruct a minor 1°–3°C cooling (Harzhauser et al., 2011; Kürschner & Kvacek, 2009) and the new reconstructions for the UK presented herein (Figures 2–6). MAP is shown to decrease between the Langhian and Serravallian but remains above the present-day UK average (Figure 6), which despite wide Co-existence Approach ranges, decreasing precipitation in the German basins is also likely (Utescher et al., 2015). Herpetological data from Central and Eastern Europe also show decreasing MAP during the Serravallian, but these are lower than the paleobotanical reconstructions (Böhme et al., 2011). Small mammal-based reconstructions show 900–1,200 mm/yr during MN7-8 (13–11.1 Ma) for most of western and central Europe that would be consistent with both the Co-existence Approach reconstructions from Germany and the new CREST and CRACLE reconstructions from the UK (van Dam, 2006). However, discrepancies between reconstructions may also be a result of age control rather than method-dependent abberations.

Within the Brassington Formation, Tortonian mean MAT reconstructions (KM-2 and KM-3, Figure 2) do not differ much from the Serravallian (KM-1, Figure 2) and are cooler than the Co-existence Approach-based reconstructions from the Lower Rhine and Weisselster basins (Pound, Haywood, et al., 2012; Pound & Riding, 2016; Utescher et al., 2015). A Late Miocene cooling is evident between the reconstructions of KM-2 and KM-3. Sample KM-3 comes from the later Tortonian (younger than 9 Ma; Pound, Riding, et al., 2012) and both CREST and N-CRACLE reconstruct a mean winter cooling of between 0.6° and 1.9°C (Figure 4). CRACLE also reconstructs a decrease in MAT of 1.6°C and a decrease in summer temperatures of ca. 2°C (Figure 2). A summer temperature decrease during the Tortonian is reconstructed from Germany, but not a winter cooling (Utescher et al., 2015). The Late Miocene Cooling (8-7 Ma) in the North Atlantic is marked by SST decreases of c. 6°C from 23°–25°C to 12°–14°C by c. 6.5 Ma (Super et al., 2020). In the Roer Valley Graben, GDGT reconstructions show a decrease in temperature of ca. 5°C between 9 and 8 Ma (Donders et al., 2009). MAP does generally decline throughout the Late Miocene with reconstructions slightly wetter than MAP reconstructions from Germany (1,150–1,300 mm; Utescher et al., 2015), ranging from >850 mm (CRACLE) to >1,500 mm (CREST) and 1,500–1,700 (Co-existence Approach; Figure 5). There may have been potentially periodic high precipitation as the CREST 2-σ confidence interval reconstructs a MAP of c. 1,850–2,300 mm during the Tortonian (Figure 5) which is within the range of the Late Miocene "washhouse events" (Böhme et al., 2011). The Roer Valley Graben record also shows the later Tortonian to be drier than earlier (Donders et al., 2009), which is consistent with the new reconstructions presented here for the UK (Figure 5).

The mean MAT values reconstructed for the Zanclean are close to the modern MAT for the UK (Figure 2). Marine assemblage based on qualitative reconstructions from the Ramsholt Member of the Coralline Crag Formation suggest a warm "Mediterranean" climate (King, 2016), whereas mollusk derived isotopic estimates of SSTs from the Coralline Crag Formation are within the cool temperate range (Vignols et al., 2019). The uncertainty on the CREST reconstructions means that they overlap with North Atlantic SSTs from ODP Site 982 of 16°–20°C and GDGT reconstructions from the Roer Valley Graben (Donders et al., 2009; Super et al., 2020). Mollusk isotope-based summer maximum surface temperature reconstructions of 17°–19°C and ostracod-based summer temperature reconstructions of 19°–21° ± 1°C compare well to our summer temperature reconstructions ranging from 12°–25°C (CREST), 15°–19°C (N-CRACLE) and 16°–18°C (Co-existence Approach; Figure 3; Tromans, 2017; Vignols et al., 2019). These values are cooler than those reconstructed for Zanclean summers in the Lower Rhine and Weisselster basins (Utescher et al., 2015). Marine proxy disagreement over winter temperatures complicates the comparison to the new paleovegetation reconstructions. The mollusk isotopic record reconstructs a winter minimum surface temperature below 10°C and possibly similar to present-day at 6°–7°C (Vignols et al., 2019) whereas the ostracod record suggests winters above 10°C and a winter range of 12–13 ± 1°C (Tromans, 2017). The new paleovegetation based reconstructions are more comparable to the mollusk isotope record, in that they are below 10°C and closer to the modern terrestrial value of 1.3°C (Figure 4). The terrestrial winter temperature reconstructed here for the Coralline Crag Formation is also comparable to the Co-existence Approach-based reconstructions from the Lower Rhine and Weisselster basins (Utescher et al., 2015). Zanclean MAP reconstructions are lower than during the Tortonian for the UK but continue to be above the modern value (Figure 5). The MAP values reconstructed here for the Zanclean of southeast England are lower than those reconstructed for the German basins but are in line with small mammal-based reconstructions (Utescher et al., 2015;

van Dam, 2006). The consistently cooler and drier reconstructions for the uppermost Zanclean sample may correspond to a glacial period, such as Marine Isotope Stage Gi4 (Lisiecki & Raymo, 2005).

There is a ca. 1°C increase in MAT from the late Zanclean to the latest Piacenzian (Figure 2). This MAT difference is probably an underestimate of Piacenzian warmth as the Red Crag Formation is post-mid Piacenzian Warm Period (Dowsett et al., 2016; Haywood, Dowsett, & Dolan, 2016). Qualitatively, the microfossil assemblage is interpreted as mild-to warm-temperate, whereas the foraminiferal and mollusk assemblages contain cool-water Pacific elements (King, 2016). In the German basins the Piacenzian has a MAT of around 14°C (Utescher et al., 2015), which is warmer than the reconstructions produced by CREST and CRACLE, but not the Co-existence Approach (Figure 2). The 2-σ uncertainty on CREST overlaps with the German Co-existence Approach reconstructions, whereas CRACLE reconstructs an MAT of around 9–10°C which is comparable to the GDGT record from the Roer Valley Graben (Donders et al., 2009). Winter temperatures were also higher in the Piacenzian than the Zanclean and the reconstructed CREST mean is comparable to the Co-existence Approach-based reconstructions from Germany (Utescher et al., 2015). CRACLE reconstructs lower winter temperatures, but still shows the increase from the Zanclean into the Piacenzian. Summer temperatures are reconstructed as lower than the Co-existence Approach-based ones from Germany (Utescher et al., 2015). North Atlantic SSTs are 14°–18°C during the time of deposition of the Red Crag Formation (Super et al., 2020), which is more comparable to the summer temperatures reconstructed here than the MAT (Figure 3). CREST and CRACLE both reconstruct a MAP of between 800 and 900 mm for the Piacenzian this is consistent with small mammal-based reconstructions but is lower than the Co-existence Approach -based reconstructions from Germany (Utescher et al., 2015; van Dam, 2006).

4.2. Model Applicability to the Miocene

There has been a reticence to apply CREST and CRACLE to pre-Quaternary scenarios, despite being recommended by DeepMIP (Hollis et al., 2019). CREST has been used in paleoclimate reconstructions of the Holocene of North and South Africa (Chase et al., 2015; Chase & Quick, 2018; Chevalier & Chase, 2015; Chevalier et al., 2017; Cordova et al., 2017; Nourelbait et al., 2016), South Korea (Yi et al., 2020), Europe (Cheddadi et al., 2016), and the Pleistocene of South Africa (Chevalier & Chase, 2016; Lim et al., 2016; Scott, 2016), Africa (Chevalier et al., 2020) and Turkey (Chevalier, 2019). CRACLE has been applied to the Holocene of North America (Lora & Ibarra, 2019) and the Pliocene of Arctic Canada (Fletcher et al., 2019). In reconstructions of Pliocene High Arctic climate using CRACLE, Fletcher et al. (2017) encountered issues with N-CRACLE estimates being uninformatively wide (e.g., −30°C to +30°C in genera-level reconstructions). The CRACLE estimates for the UK Neogene climate are not uninformatively wide despite using mostly genera- and family level identifications (Data Set S3). This might imply that, like the Co-existence Approach, CRACLE performs better at midlatitudes than it does at higher latitudes (Pound & Salzmann, 2017; Utescher et al., 2014). However, Klages et al. (2020) applied a NLR-based *pdf* technique to the Cretaceous of the Antarctic and achieved reconstructions comparable to independent geochemical palaeothermometry.

The most obvious disparity in our results between N-CRACLE and P-CRACLE is for the trends in MAP and precipitation seasonality (Figures 5 and 6). However, it occurs only from the Middle to Late Miocene with N-CRACLE estimating a wetter MAP of c. 650 mm (Figure 5). N-CRACLE results for the Trwyn y Parc sample are more in line with CREST and the Co-existence Approach, whilst P-CRACLE is significantly lower (Figure 5). The fact that N-CRACLE makes no assumption of normal distribution in the overlapping climate spaces of the taxa means it is more applicable to older samples where a non-modern analogue vegetation is highly probable (Klages et al., 2020). However, N-CRACLE seasonality then differs from CREST, but is comparable to the trend reconstructed by the Co-existence Approach (Figure 6).

Overall, CREST and CRACLE both produce paleoclimatic values and trends for the UK comparable to, but lower than, the Co-existence Approach. The reconstructed values and trends also show comparability to independent records from northwest Europe and the Atlantic Ocean. They have the advantage over the widely used Co-existence Approach that they produce statistical uncertainty that will make proxy-proxy and data-model comparisons more robust (Haywood, Dowsett, Dolan, et al., 2016; Hollis et al., 2019). However, as a nearest living relative technique, they still come with widely acknowledged limitations (Grimm et al., 2016; Utescher et al., 2014) and are unable to reconstruct paleoclimates warmer than the warmest modern climate space.

4.3. Implications for Future Climate Change

Although no geological time period is a perfect analogue for future anthropogenic warming, both the Miocene and the Pliocene have been proposed as imperfect analogues (Burke et al., 2018; Steinthorsdottir et al., 2021). The UK is predicted to experience MAT increases by the period 2080–2099 of 0.3°–2.6°C under scenario Representative Concentration Pathway (RCP) 2.6 and MAT increases of 1.9°–6.3°C for emissions scenario RCP8.5 (Lowe et al., 2018). For the Pliocene, CRACLE reconstructs warming within the range of RCP2.6, whilst the Miocene reconstructions from both CREST and CRACLE are in line with RCP8.5 warming (Figure 2). The Pliocene was the most recent geological interval with atmospheric CO_2 at, or above 400 ppm (Burke et al., 2018). The Miocene has a more variable CO_2 reconstruction, but the Late Miocene is considered to 350–500 ppm and the Middle Miocene 400–600+ ppm (Steinthorsdottir et al., 2021). Reconstructed Pliocene winter temperatures are in line with projected increases associated with the RCP2.6 and the 50th percentile for RCP4.5, whilst the Miocene reconstructions are comparable to the 90th percentile for RCP4.5, all percentiles of RCP6.0 and the 50th percentile for RCP8.5 (Lowe et al., 2018). However, reconstructed summer temperatures do not differ much from modern values until the Serravallian and Langhian (Figure 3). The Serravallian summer warming is comparable to the 50th percentile projections for RCP2.6–RCP6.0, whilst the Langhian potentially shows summer warming equivalent to RCP8.5 in the UK (Lowe et al., 2018). The UK has already seen increases in MAP over the last few decades (Lowe et al., 2018) and the Pliocene reconstructions, considered an analogue for near-term future climate by Burke et al. (2018), have MAP values 28.4%–84.5% higher than the modern values for southeast England (Figure 5). The Late Miocene values are closer to modern values with only a potential increase of 7% on the modern value for upland central England, whilst the Langhian reconstructions are 45% lower for P-CRA-CLE, but 35.6%–61.6% higher for CREST and N-CRACLE (Figure 5). Precipitation seasonality is predicted to increase under future climate change with wetter winters and drier summers for the UK (Lowe et al., 2018). All reconstructions show seasonality higher than modern during the Neogene of the UK, except for the P-CRACLE reconstruction of the Langhian.

5. Conclusions

The new probability-based terrestrial Neogene climate reconstruction of the UK shows a cooling trend from the Langhian to the Pliocene-Pleistocene boundary. During the Langhian the UK was up to 6°C warmer than present day and this was accompanied by warmer winters and summers. During the Serravallian and early Tortonian the UK continued to be around 3°–4°C warmer than today, but late Miocene cooling resulted in the UK during the late Tortonian and Pliocene being only 1.0°–2.9°C warmer. Although neither of the Pliocene sections contain the mid-Piacenzian Warm Period these differences with present-day are lower than previous reconstructions using the Co-existence Approach, but in line with independent proxy reconstructions from the wider region. MAP was potentially 161% modern during the Langhian a period considered an Interval of Interest for future anthropogenic warming by IPCC 6 (IPCC, 2021). MAP is also consistently higher in all Pliocene samples, despite them not coming from the warmest and wettest interval of the Pliocene. Overall, CREST and CRACLE produce trends and values consistent with both the Co-existence Approach and independent palaeoclimate data. For non-analogue vegetation, in our study of the Langhian, the use of N-CRACLE is recommended.

Data Availability Statement

The taxa lists, list of NLRs used, CREST, CRACLE, and Co-existence Approach results used in the paleoclimate reconstruction in this study are available at Zenodo (https://doi.org/10.5281/zenodo.5813639; CC-BY: Creative Commons Attribution 4.0 International). Code to repeat data downloads with current versions of these databases can be found via the following links. All analyses were carried out using R software (R Core Team, 2021). The "CREST" code and documentation are available at GitHub (https://github.com/mchevalier2/crestr). The "cRacle" package is distributed under an MIT License, and all code and documentation are available on GitHub via the original repository (https://www.github.com/rsh249/cRacle). Minor amendments were applied to the original code: adjusting the number of maximum records used when retrieving climate data and using an optcosine kernel density function. The amended code is available at GitHub (https://github.com/martha-gibson/cRacle) and Zenodo (https://doi.org/10.5281/zenodo.5702602).

References

Andrew, R., & West, R. G. (1977). Pollen spectra from Pliocene crag at Orford, Suffolk. *New Phytologist*, *78*, 709–714. https://doi.org/10.1111/j.1469-8137.1977.tb02175.x

Balson, P. S. (1999a). The Neogene of eastern England. In B. Daley, & P. Balson (Eds.), *British tertiary stratigraphy*. (pp. 235–241), Joint Nature Conservancy Committee.

Balson, P. S. (1999b). The Coralline Crag. In B. Daley, & P. Balson (Eds.), *British tertiary stratigraphy*. (pp. 255–288), Peterborough: Joint Nature Conservancy Committee.

Böhme, M. (2004). Migration history of air-breathing fishes reveal Neogene atmospheric circulation pattern. *Geology*, *32*, 393–396. https://doi.org/10.1130/G20316.1

Böhme, M., Winklhofer, M., & Ilg, A. (2011). Miocene precipitation in Europe: Temporal, trends and spatial gradients. *Palaeogeography, Palaeoclimatology, Palaeoecology*, *304*, 212–218. https://doi.org/10.1016/j.palaeo.2010.09.028

Bruch, A. A., Utescher, T., & Mosbrugger, V. (2011). Precipitation patterns in the Miocene of Central Europe and the development of continentality. *Palaeogeography, Palaeoclimatology, Palaeoecology*, *304*(3–4), 202–211. https://doi.org/10.1016/j.palaeo.2010.10.002

Burke, K. D., Williams, J. W., Chandler, M. A., Haywood, A. M., Lunt, D. J., & Otto-Bliesner, B. L. (2018). Pliocene and Eocene provide best analogs for near-future climates. *Proceedings of the National Academy of Sciences of the United States of America*, *115*(52), 13288–13293. https://doi.org/10.1073/pnas.1809600115

Burls, N. J., Bradshaw, C. D., De Boer, A. M., Herold, N., Huber, M., Pound, M., et al. (2021). Simulating Miocene warmth: Insights from an opportunistic multi-model ensemble (MioMIP1). *Paleoceanography and Paleoclimatology*, *36*, e2020PA004054. https://doi.org/10.1029/2020PA004054

Chase, B. M., Boom, A., Carr, A. S., Carré, M., Chevalier, M., Meadows, M. E., et al. (2015). Evolving southwest African response to abrupt deglacial North Atlantic climate change events. *Quaternary Science Reviews*, *121*, 132–136. https://doi.org/10.1016/j.quascirev.2015.05.023

Chase, B. M., & Quick, L. J. (2018). Influence of Agulhas forcing of Holocene climate change in South Africa's southern Cape. *Quaternary Research*, *90*(2), 303–309. https://doi.org/10.1017/qua.2018.57

Cheddadi, R., Araújo, M. B., Maiorano, L., Edwards, M., Guisan, A., Carré, M., et al. (2016). Temperature range shifts for three European tree species over the last 10,000 years. *Frontiers in Plant Science*, *7*, 1581. https://doi.org/10.3389/fpls.2016.01581

Chevalier, M. (2019). Enabling possibilities to quantify past climate from fossil assemblages at a global scale. *Global and Planetary Change*, *175*, 27–35. https://doi.org/10.1016/j.gloplacha.2019.01.016

Chevalier, M., Brewer, S., & Chase, B. M. (2017). Qualitative assessment of PMIP3 rainfall simulations across the eastern African monsoon domains during the mid-Holocene and the Last Glacial Maximum. *Quaternary Science Reviews*, *156*, 107–120. https://doi.org/10.1016/j.quascirev.2016.11.028

Chevalier, M., & Chase, B. M. (2015). Southeast African records reveal a coherent shift from high- to low-latitude forcing mechanisms along the east African margin across last glacial–interglacial transition. *Quaternary Science Reviews*, *125*, 117–130. https://doi.org/10.1016/j.quascirev.2015.07.009

Chevalier, M., & Chase, B. M. (2016). Determining the divers of long-term aridity variability: A southern African case study. *Journal of Quaternary Science*, *31*(2), 143–151. https://doi.org/10.1002/jqs.2850

Chevalier, M., Chase, B. N., Quick, L. J., Dupont, L. M., & Johnson, T. C. (2020). Temperature change in subtropical southeastern Africa during the past 790,000 yr. *Geology*, *49*(1), 71–75. https://doi.org/10.1130/G47841.1

Chevalier, M., Cheddadi, R., & Chase, B. M. (2014). CREST (Climate REconstruction SofTware): A probability density function (PDF)-based quantitative climate reconstruction method. *Climate of the Past*, *10*, 2081–2098. https://doi.org/10.5194/cp-10-2081-2014

Cordova, C. E., Scott, L., Chase, B. M., & Chevalier, M. (2017). Late pleistocene-holocene vegetation and climate change in the middle Kalahari, lake Ngami, Botswana. *Quaternary Science Reviews*, *171*, 199–215. https://doi.org/10.1016/j.quascirev.2017.06.036

Davies, N. S., Shillito, A. P., & McMahon, W. J. (2019). Where does the time go? Assessing the chronostratigraphic fidelity of sedimentary geological outcrops in the Pliocene-Pleistocene Red Crag Formation, eastern England. *Journal of the Geological Society*, *176*, 1154–1168. https://doi.org/10.1144/jgs2019-056

Denk, T., Grimm, G. W., Grimsson, F., & Zetter, R. (2013). Evidence from "Köppen signatures" of fossil plant assemblages from effective heat transport of Gulf Stream to subarctic North Atlantic during Miocene cooling. *Biogeosciences*, *10*, 7927–7942. https://doi.org/10.5194/bg-10-7927-2013

De Schepper, S., Head, M. J., & Louwye, S. (2008). Pliocene dinoflagellate cyst stratigraphy, palaeoecology and sequence stratigraphy of the Tunnel-Canal Dock, Belgium. *Geological Magazine*, *146*(1), 92–112. https://doi.org/10.1017/S0016756808005438

Donders, T. H., Weijers, J. W. H., Munsterman, D. K., Kloosterboer-van Hoeve, M. L., Buckles, L. K., Pancost, R. D., et al. (2009). Strong climate coupling of terrestrial and marine environments in the Miocene of northwest Europe. *Earth and Planetary Science Letters*, *281*, 215–225. https://doi.org/10.1016/j.epsl.2009.02.034

Dowsett, H., Dolan, A., Rowley, D., Moucha, R., Forte, A. M., Mitrovica, J. X., et al. (2016). The PRISM4 (mid-Piacenzian) paleoenvironmental reconstruction. *Climate of the Past*, *12*, 1519–1538. https://doi.org/10.5194/cp-12-1519-2016

Eronen, J. T., Micheels, A., & Utescher, T. (2012). A comparison of estimates of mean annual precipitation from different proxies: A pilot study of the European Neogene. *Evolutionary Ecology Research*, *13*, 851–867.

Fick, S. E., & Hijmans, R. J. (2017). WorldClim 2: New 1km spatial resolution climate surfaces for global land areas. *International Journal of Climatology*, *37*(12), 4302–4315. https://doi.org/10.1002/joc.5086

Fletcher, T., Feng, R., Telka, A. M., Matthews, J. V., Jr, & Ballantyne, A. (2017). Floral dissimilarity and the influence of climate in the Pliocene High Arctic: Biotic and abiotic influences on five sites on the Canadian Arctic Archipelago. *Frontiers in Ecology and Evolution*, *5*. https://doi.org/10.3389/fevo.2017.00019

Fletcher, T. L., Csank, A. Z., & Ballantyne, A. P. (2019). Identifying bias in cold season temperature reconstructions by beetle mutual climatic range methods in the Pliocene Canadian High Arctic. *Palaeogeography, Palaeoclimatology, Palaeoecology*, *514*, 672–676. https://doi.org/10.1016/j.palaeo.2018.11.025

GBIF. (2021). *GBIF Home Page*. Retrieved from https://www.gbif.org

Grimm, G. W., Bouchal, J. M., Denk, T., & Potts, A. (2016). Fables and foibles: A critical analysis of the Palaeoflora database and the co-existence approach for palaeoclimate reconstruction. *Review of Palaeobotany and Palynology*, *233*, 216–235. https://doi.org/10.1016/j.revpalbo.2016.07.001

Grimm, G. W., & Potts, A. J. (2016). Fallacies and fantasies: The theoretical underpinnings of the Coexistence Approach for palaeoclimate reconstruction. *Climate of the Past*, *12*, 611–622. https://doi.org/10.5194/cp-12-611-2016

Hall, A. M., Gilg, H. A., Fallick, A. E., & Merritt, J. W. (2015). Kaolins in gravels and saprolites in north-east Scotland: Evidence from stable H and O isotopes for Palaeocene-Miocene deep weathering. *Palaeogeography, Palaeoclimatology, Palaeoecology*, *424*, 6–16. https://doi.org/10.1016/j.palaeo.2015.02.019

Harbert, R. S., & Baryiames, A. A. (2020). cRacle: R tools for estimating climate from vegetation. *Applications in Plant Sciences*, *8*(2), e11322. https://doi.org/10.1002/aps3.11322

Harbert, R. S., & Nixon, K. C. (2015). Climate reconstruction analysis using coexistence likelihood estimation (CRACLE): A method for the estimation of climate using vegetation. *American Journal of Botany*, *102*(8), 1277–1289. https://doi.org/10.3732/ajb.1400500

Harzhauser, M., & Piller, W. E. (2007). Benchmark data of a changing sea—Palaeogeography, palaeobiogeography and events in the Central Paratethys during the Miocene. *Palaeogeography, Palaeoclimatology, Palaeoecology*, *253*, 8–31. https://doi.org/10.1016/j.palaeo.2007.03.031

Harzhauser, M., Piller, W. E., Müllegger, S., Grunert, P., & Micheels, A. (2011). Changing seasonality patterns in Central Europe from Miocene Climate optimum to Miocene climate transition deduced from the Crassostrea isotope archive. *Global and Planetary Change*, *76*, 77–84. https://doi.org/10.1016/j.gloplacha.2010.12.003

Haywood, A. M., Dowsett, H. J., & Dolan, A. M. (2016). Integrating geological archives and climate models for the mid-Pliocene warm period. *Nature Communications*, *7*(1), 1–14. https://doi.org/10.1038/ncomms10646

Haywood, A. M., Dowsett, H. J., Dolan, A. M., Rowley, D., Abe-Ouchi, A., Otto-Bliesner, B., et al. (2016). The Pliocene model Intercomparison Project (PlioMIP) phase 2: Scientific objectives and experimental design. *Climate of the Past*, *12*(3), 663–675. https://doi.org/10.5194/cp-12-663-2016

Head, M. J. (1997). Thermophilic dinoflagellate assemblages from the mid Pliocene of eastern England. *Journal of Paleontology*, *71*(2), 165–193. https://doi.org/10.1017/S0022336000039123

Head, M. J. (1998). Pollen and dinoflagellates from the Red Crag at Walton-on-the-Naze, Essex: Evidence for a mild climatic phase during the early late Pliocene of eastern England. *Geological Magazine*, *135*(6), 803–817. https://doi.org/10.1017/s0016756898001745

Herbert-Smith, M. (1971). *Palynology of the tertiary and Pleistocene deposits of the Llanbedr (Mochras Farm) borehole*. In A. Woodland (Ed.), (pp. 95–105). Report of the Institute of the Geological Sciences.

Holbourn, A., Kuhnt, W., Kochhann, K. G. D., Andersen, N., & Meier, K. J. S. (2015). Global perturbation of the carbon cycle at the onset of the Miocene climatic optimum. *Geology*, *43*, 123–126. https://doi.org/10.1130/g36317.1

Hollis, C. J., Dunkley Jones, T., Anagnostou, E., Bijl, P. K., Cramwinckel, M. J., Cui, Y., et al. (2019). The DeepMIP contribution to PMIP4: Methodologies for selection, compilation and analysis of latest Paleocene and early Eocene climate proxy data, incorporating version 0.1 of the DeepMIP database. *Geoscientific Model Development*, *12*(7), 3149–3206. https://doi.org/10.5194/gmd-12-3149-2019

IPCC. (2021). *Climate change 2021: The physical science basis. Contribution of working group I to the sixth assessment report of the intergovernmental panel on climate change*. In V. Masson-Delmotte, P. Zhai, A. Pirani, S. L. Connors, C. Péan, S. Berger, et al. (Eds.), Cambridge University Press. Retrieved from https://www.ipcc.ch/report/ar6/wg1/

Jaques, F. M. B., Guo, S.-X., Su, T., Xing, Y.-W., Huang, Y.-J., Liu, Y.-S., et al. (2011). Quantitative reconstruction of the late Miocene monsoon climates of southwest China: A case study of the Lincang flora from Yunnan Province. *Palaeogeography, Palaeoclimatology, Palaeoecology*, *304*, 318–327. https://doi.org/10.1016/j.palaeo.2010.04.014

King, C. (2016). A revised correlation of Tertiary rocks in the British Isles and adjacent areas of NW Europe. In A. S. Gale, & T. L. Barry (Eds.), *Geological Society, London, Special Reports* (Vol. 27, pp. 269–327). Retrieved From www.geolsoc.org.uk/SR027

Klages, J. P., Salzmann, U., Bickert, T., Hillenbrand, C. D., Gohl, K., Kuhn, G., et al. (2020). Temperate rainforests near the South Pole during peak Cretaceous warmth. *Nature*, *580*(7801), 81–86. https://doi.org/10.1038/s41586-020-2148-5

Kürschner, W. M., & Kvacek, Z. (2009). Oligocene-Miocene CO_2 fluctuations, climatic and palaeofloristic trends inferred from fossil plant assemblages in central Europe. *Bulletin of Geosciences*, *84*, 189–202. https://doi.org/10.3140/bull.geosci.1091

Lear, C. H., Coxall, H. K., Foster, G. L., Lunt, D. J., Mawbey, E. M., Rosenthal, Y., et al. (2015). Neogene ice volume and ocean temperatures: Insights from infaunal foraminiferal Mg/Ca paleothermometry. *Paleoceanography*, *30*, 1437–1454. https://doi.org/10.1002/2015PA002833

Lee, J. R., Candy, I., & Haslam, R. (2018). The Neogene and Quaternary of England: Landscape evolution, tectonics, climate change and their expression in the geological record. *Proceedings of the Geologists' Association*, *129*, 452–481. https://doi.org/10.1016/j.pgeola.2017.10.0030016-7878

Levy, R., Harwood, D., Florindo, F., Sandiorgi, F., Tripati, R., von Eynatten, H., et al. (2016). Antarctic ice sheet sensitivity to atmospheric CO_2 variations in the early to mid-Miocene. *Proceedings of the National Academy of Sciences*, *113*, 3453–3458. https://doi.org/10.1073/pnas.1516030113

Lim, S., Chase, B. M., Chevalier, M., & Reimer, P. J. (2016). 50,000 years of vegetation and climate change in the southern Namib Desert, Pella, South Africa. *Palaeogeography, Palaeoclimatology, Palaeoecology*, *451*, 197–209. https://doi.org/10.1016/j.palaeo.2016.03.001

Lisiecki, L. E., & Raymo, M. E. (2005). A Pliocene-Pleistocene stack of 57 globally distributed benthic δ18O records. *Paleoceanography*, *20*(1). https://doi.org/10.1029/2004PA001071

Lora, J. M., & Ibarra, D. E. (2019). The North American hydrological cycle through the last deglaciation. *Quaternary Science Reviews*, *226*, 105991. https://doi.org/10.1016/j.quascirev.2019.105991

Lowe, J. A., Bernie, D., Bett, P., Bricheno, L., Brown, S., Calvert, D., et al. (2018). *UKCP18 science overview report*. Met Office Hadley Centre. Retrieved from https://www.metoffice.gov.uk/pub/data/weather/uk/ukcp18/science-reports/UKCP18-Overview-report.pfd

Methner, K., Campani, M., Fiebig, J., Löffler, N., Kempf, O., & Mulch, A. (2020). Middle Miocene long-term continental temperature change in and out of pace with marine climate records. *Scientific Reports*, *10*, 7989. https://doi.org/10.1038/s41598-020-64743-5

Mosbrugger, V., & Utescher, T. (1997). The coexistence approach—A method for quantitative reconstructions of Tertiary terrestrial palaeoclimate data using plant fossils. *Palaeogeography, Palaeoclimatology, Palaeoecology*, *134*, 61–86. https://doi.org/10.1016/S0031-0182(96)00154-X

Mosbrugger, V., Utescher, T., & Dilcher, D. L. (2005). Cenozoic continental climatic evolution of Central Europe. *Proceedings of the National Academy of Sciences*, *102*, 14964–14969. https://doi.org/10.1073/pnas.0505267102

Nourelbait, M., Rhoujjati, A., Benkaddour, A., Carré, M., Eynaud, F., Martinez, P., et al. (2016). Climate change and ecosystems dynamics over the last 6000 years in the Middle Atlas, Morocco. *Climate of the Past*, *12*, 1029–1042. https://doi.org/10.5194/cp-12-1029-2016

Popova, S., Utescher, T., Gromyko, D. V., Bruch, A. A., & Mosbrugger, V. (2012). Palaeoclimate evolution in Siberia and the Russian far east from the Oligocene to Pliocene—Evidence from fruit and seed floras. *Turkish Journal of Earth Sciences*, *21*, 315–334. https://doi.org/10.3906/yer-1005-6

Popova, S., Utescher, T., Gromyko, D. V., Mosbrugger, V., Herzog, E., & Francois, L. (2013). Vegetation change in Siberia and the northeast of Russia during the Cenozoic cooling: A study based on diversity of plant functional types. *Palaios*, *28*, 418–432. https://doi.org/10.2110/palo.2012.p12-096r

Pound, M., & McCoy, J. (2021). A new palaeoclimate reconstruction and age assessment of the Miocene Trwyn y Parc solution pipe complex on Anglesey, Wales. *Palynology*, 1–21. https://doi.org/10.1080/01916122.2021.1916636

Pound, M., & Riding, J. B. (2016). Palaeoenvironment, palaeoclimate and age of the Brassington Formation (Miocene) of Derbyshire, UK. *Journal of the Geological Society*, *163*, 306–319. https://doi.org/10.1144/jgs2015-050

Pound, M. J., Haywood, A. M., Salzmann, U., & Riding, J. B. (2012). Global vegetation dynamics and latitudinal temperature gradients during the mid to late Miocene (15.97–5.33 Ma). *Earth-Science Reviews*, *112*, 1–22. https://doi.org/10.1016/j.earscirev.2012.02.005

Pound, M. J., Riding, J. B., Donders, T. H., & Dašková, J. (2012). The palynostratigraphy of the Brassington Formation (upper Miocene) of the southern Pennines, central England. *Palynology*, *36*(1), 26–37. https://doi.org/10.1080/01916122.2011.643066

Pound, M. J., & Salzmann, U. (2017). Heterogeneity in global vegetation and terrestrial climate change during the late Eocene to early Oligocene transition. *Scientific Reports*, *7*, 43386. https://doi.org/10.1038/srep43386

Quaijtaal, W., Donders, T. H., Persico, D., & Louwye, S. (2014). Characterising the middle Miocene Mi-events in the Eastern North Atlantic realm: A first high-resolution marine palynological record from the Porcupine Basin. *Palaeogeography, Palaeoclimatology, Palaeoecology*, *399*, 140–159. https://doi.org/10.1016/j.palaeo.2014.02.017

Quan, C., Liu, Y.-S., Tang, H., & Utescher, T. (2014). Miocene shift of European atmospheric circulation from trade wind to westerlies. *Scientific Reports*, *4*. https://doi.org/10.1038/srep05660

R Core Team. (2021). *R: A language and environment for statistical computing*. R Foundation for Statistical Computing. Retrieved from https://www.R-project.org

Riding, J. B., Head, M. J., & Moorlock, B. S. P. (2000). Reworked palynomorphs from the Red Crag and Norwich Crag formations (early Pleistocene) of the Ludham Borehole, Norfolk. *Proceedings of the Geological Association*, *111*, 161–171. https://doi.org/10.1016/S0016-7878(00)80006-1

Rohli, R. V., & Vega, A. J. (2008). *Climatology*. (pp. 467). Jones and Bartlett Publishers.

Salzmann, U., Dolan, A. M., Haywood, A. M., Chan, W. -L., Voss, J., Hill, D. J., et al. (2013). Challenges in quantifying Pliocene terrestrial warming revealed by data-model discord. *Nature Climate Change*, *3*, 969–974. https://doi.org/10.1038/nclimate2008

Scott, L. (2016). Fluctuations of vegetation and climate over the last 75 000 years in the Savanna Biome, South Africa: Tswaing Crater and Wonderkrater pollen sequences reviewed. *Quaternary Science Reviews*, *145*, 117–133. https://doi.org/10.1016/j.quascirev.2016.05.035

Shevenell, A. E., Kennett, J. P., & Lea, D. W. (2008). Middle Miocene ice sheet dynamics, deep-sea temperatures, and carbon cycling: A southern ocean perspective. *Geochemistry, Geophysics, Geosystems*, *9*, Q02006. https://doi.org/10.1029/2007GC001736

Steinthorsdottir, M., Coxall, H. K., de Boer, A. M., Huber, M., Barbolini, N., Bradshaw, C. D., et al. (2021). The Miocene: The future of the past. *Paleoceanography and Paleoclimatology*, *36*, e2020PA004037. https://doi.org/10.1029/2020PA004037

Super, J. R., Thomas, E., Pagani, M., Huber, M., O'Brien, C., & Hull, P. M. (2018). North Atlantic temperature and pCO_2 coupling in the early-middle Miocene. *Geology*, *46*(6), 519–522. https://doi.org/10.1130/G40228.1

Super, J. R., Thomas, E., Pagani, M., Huber, M., O'Brien, C. L., & Hull, P. M. (2020). Miocene evolution of north Atlantic Sea surface temperature. *Paleoceanography and Paleoclimatology*, *35*, e2019PA003748. https://doi.org/10.1029/2019PA003748

Tromans, D. (2017). *Pliocene global warming: An ostracodal and sedimentological analysis of the Coralline Crag Formation*. Retrieved from http://curve.coventry.ac.uk/open/items/92c26ee6-0278-49df-8afd-5b8d0d2ba558/1/

Utescher, T., Bondarenko, O. V., & Mosburger, V. (2015). The Cenozoic Cooling—Continental signals from the Atlantic and Pacific side of Eurasia. *Earth and Planetary Science Letters*, *415*, 121–133. https://doi.org/10.1016/j.epsl.2015.01.019

Utescher, T., Bruch, A. A., Erdei, B., François, L., Ivanov, D., Jacques, F. M. B., et al. (2014). The coexistence approach—Theoretical background and practical considerations of using plant fossils for climate quantification. *Palaeogeography, Palaeoclimatology, Palaeoecology*, *410*, 58–73. https://doi.org/10.1016/j.palaeo.2014.05.031

Utescher, T., Erdei, D., Hably, L., & Mosbrugger, V. (2017). Late Miocene vegetation of the Pannonian basin. *Palaeogeography, Palaeoclimatology, Palaeoecology*, *467*, 131–148. https://doi.org/10.1016/j.palaeo.2016.02.042

van Dam, J. A. (2006). Geographic and temporal patterns in the late Neogene (12–3 Ma) aridification of Europe: The use of small mammals as paleoprecipitation proxies. *Palaeogeography, Palaeoclimatology, Palaeoecology*, *238*, 190–218. https://doi.org/10.1016/j.palaeo.2006.03.025

Vignols, R. M., Valentine, A. M., Finlayson, A. G., Harper, E. M., Schöne, B. R., Leng, M. J., et al. (2019). Marine climate and hydrography of the Coralline Crag (early Pliocene, UK): Isotopic evidence from 16 benthic invertebrate taxa. *Chemical Geology*, *526*, 62–83. https://doi.org/10.1016/j.chemgeo.2018.05.034

Vines, R. G. (1985). European rainfall patterns. *Journal of Climatology*, *5*(6), 607–616. https://doi.org/10.1002/joc.3370050603

Walsh, P. T., Atkinson, K., Boulter, M. C., & Shakesby, R. A. (1987). The Oligocene and Miocene outliers of west Cornwall and their Bearing on the geomorphological evolution of Oldland Britain. *Philosophical Transactions of the Royal Society of London. Series A, Mathematical and Physical Sciences*, *323*, 211–245. https://doi.org/10.1098/rsta.1987.0082

Walsh, P. T., Banks, J. V., Jones, P. F., Pound, M. J., & Riding, J. B. (2018). A reassessment of the Brassington Formation (Miocene) of Derbyshire, UK and a review of related hypogene karst suffosion processes. *Journal of the Geological Society*, *175*(3), 443–463. https://doi.org/10.1144/jgs2017-029

Walsh, P. T., Morawiecka, I., & Skawinaska-Wieser, K. (1996). A Miocene palynoflora preserved by karstic subsidence in Anglesey and the origin of the Menaian Surface. *Geological Magazine*, *133*, 713–719. https://doi.org/10.1017/S0016756800024560

Williams, M., Haywood, A. M., Hjarper, E. M., Johnson, A. L., Knowles, T., Leng, M. J., et al. (2009). Pliocene climate and seasonality in North Atlantic shelf seas. *Philosophical Transactions of the Royal Society A*, *367*, 85–108. https://doi.org/10.1098/rsta.2008.0224

Wood, A. M. (2012). An Arctic ostracod fauna from the pre-Ludhamian (late Pliocene to early Pleistocene) Red Crag Formation at Buckanay Farm, Suffolk, England. In R. Dixon (Ed.), *A Celebration of Suffolk Geology, GeoSuffolk, Ipswich* (pp. 199–214). Retrieved from https://www.researchgate.net/publication/262827019_An_Arctic_ostracod_fauna_from_the_Pre-Ludhamian_late_Pliocene_to_early_Pleistocene_Red_Crag_Formation_at_Buckanay_Farm_Suffolk_England

Wood, A. M., Whatley, R., Cronin, T. M., & Holtz, T. R. (1993). Pliocene paleotemperature reconstruction for the southern North Sea based on Ostracoda. *Quaternary Science Reviews*, *12*(9), 747–767. https://doi.org/10.1016/0277-3791(93)90015-E

Yi, S., Jun, C. P., Jo, K. N., Lee, H., Kim, M.-S., Lee, S. D., et al. (2020). Asynchronous multi-decadal time-scale series of biotic and abiotic responses to precipitation during the last 1300 years. *Scientific Reports*, *10*, 17814. https://doi.org/10.1038/s41598-020-74994-x